

Synthesis of Eu^{3+} -doped ZnONanocomposite for Photocatalytic Degradation of Methylene blue dye



GenaNura

**A Thesis Submitted to the Department of Applied Chemistry
College of Applied Natural Science**

**Presented in Partial Fulfillment of the Requirement for the Degree of Master's in
Applied Chemistry (Industrial Chemistry)**

**Office of Graduate Studies
Adama Science and Technology University**

**Dec, 2025
Adama, Ethiopia**

**Synthesis of Eu³⁺-doped ZnO Nanocomposite for Photocatalytic Degradation of
Methylene blue dye**

GenaNura

Supervisor: Gemechu Deressa (Ph.D.)

A Thesis Submitted to the Department of Applied Chemistry,
College Applied Natural science

Presented in Partial Fulfillment of the Requirement for the Degree of Master's in Applied
Chemistry (Industrial Chemistry)

Office of Graduate Studies
Adama Science and Technology University

Dec, 2025
Adama, Ethiopia

DECLARATION

I hereby declare that this Master Thesis entitled “**Synthesis of Eu³⁺-doped ZnO Nanocomposite for Photocatalytic Degradation of Methylene blue dye**” is my original work. That is, it has not been submitted for the award of any academic degree, diploma or certificate in any other university. All sources of materials that are used for this thesis have been duly acknowledged through citation

Gena Nura

Name of student

Signature

Date

Recommendation of Advisors/ Supervisors:

I, the major advisor of this thesis, hereby certify that we have read the revised version of the thesis entitled “**Synthesis of Eu³⁺-doped ZnO Nanocomposite for Photocatalytic Degradation of Methylene blue dye**” prepared under my/our guidance by **GenaNura** submitted in partial fulfillment of the requirements for the degree of Masters of Science in Applied Chemistry (Industrial Chemistry). Therefore, we recommend the submission of revised version of the thesis to the department following the applicable procedures.

Gemmechu Deressa (Ph.D.)
Major Advisor/Supervisor

Signature

Date

APPROVAL SHEET

I, the advisor of the thesis entitled “**Synthesis of Eu³⁺-doped ZnO Nanocomposite for Photocatalytic Degradation of Methylene blue dye**” and developed by **GenaNura**, hereby certify that the recommendation and suggestions made by the board of examiners are appropriately incorporated into the final version of the thesis.

Gemmechu Deressa (Ph.D.)

Major Advisor/Supervisor

Signature

Date

We, the undersigned, members of the Board of Examiners of the thesis by **Gena Nura** have read and evaluated the thesis entitled “**Synthesis of Eu³⁺-doped ZnO Nanocomposite for Photocatalytic Degradation of Methylene blue dye**” and examined the candidate during open defense. This is, therefore, to certify that the thesis is accepted for partial fulfillment of the requirement of the degree of Master of Science in Applied Chemistry (Industrial Chemistry).

Chairperson

Signature

Date


Internal Examiner

Signature

Date

Dr. Ali Mohammed

External Examiner


Signature

Dec. 26/2025

Date

Final approval and acceptance of the thesis is contingent upon submission of its final copy to the Office of Postgraduate Studies (OPGS) through the Department Graduate Council (DGC) and College Graduate Committee (CGC).

Department Head

Signature

Date

College Dean

Signature

Date

Office of Postgraduate Studies, Dean

Signature

Date

ACKNOWLEDGEMENTS

First and foremost, I would like to thank Almighty Allah for giving health to do this work. To him alone, I ascribe all the glory. I sincerely acknowledge my hard-working advisors, **Dr. Gemechu Deressa** for his crucial remarks, valuable support and appreciable guidance, and comments in every step of this work. I appreciate the time he devoted to this work and his experience. It is a great privilege and honor for me to be advised by him. I would also to say thanks to lab Assistant **Mr. Guta Amenu** for his encouragement and support. Last but not least, I would like to extend my most profoundly gratitude to my curious mother Jano Rorisa I friendly Mr.Ahmed Kemer and his wife Hadise Mohammed, Mr.Ahmed Kassahun Yibre Mr. Jemal Keno Gobena, to all my beloved family icon and backbone of our life my wife Mrs Sifan Alkedir Abdurahaman for their sincere love, help and encouragement during the entire study period.

TABLE OF CONTENTS

DECLARATION	ii
APPROVAL SHEET	iv
ACKNOWLEDGEMENTS	v
LIST OF FIGURES	viii
LIST OF ACRONYMS	ix
ABSTRACT	i
INTRODUCTION	1
1.1. Background of Study	1
1.2. Statement of the problem	3
1.3. Objective of the study	4
1.3.1. General objective	4
1.3.2. Specific objective	4
1.4. Significance of the study	4
1.5. Scope of the study	4
CHAPTER TWO	5
LITERATURE REVIEW	5
2.1. The pollution of water	5
2.1.1. Properties of methylene blue (MB) dye	6
2.1.2. Methods used to remove MB from water	7
2.2. Introduction to nanotechnology and nanomaterials	8
2.3. Nanoparticles (NPs)	9
2.3.1. Zinc oxide (ZnO) nanoparticles	9
2.4. Photocatalysis	10
2.4.1. Mechanism of photocatalytic degradation	10
2.5. Doping	11
2.6. Synthesis methods	13

CHAPTER THREE	15
MATERIALS AND METHODS	15
3.1. Experimental site	15
3.2. Chemicals and reagents	15
3.3. Equipment and instruments	15
3.4. Synthesis of photocatalysts	15
3.5. Characterization of as synthesized photocatalysts	17
3.5.1. X-Ray diffraction (XRD)	17
3.5.2. UV-Vis DRS	17
3.5.3. Photoluminescence (PL)	17
3.5.4. Fourier transform infrared spectroscopy (FT-IR)	18
3.6. Photocatalytic degradation of Methylene blue studies	18
3.6.1. Effect of some operational parameter	18
CHAPTER FOUR	19
RESULT AND DISCUSSION	19
4.1. X-Ray diffraction (XRD) pattern analysis	19
4.2. UV Visible-DRS analysis	20
4.3. Photoluminescence (PL)	22
4.4. Fourier-Transform Infrared Spectroscopy (FTIR) Analysis	23
4.5. Photocatalytic activities	24
4.5.2. Dosage effect	27
CHAPTER FIVE	30
CONCLUSION AND RECOMMENDATION	30
5.1. Conclusion	30
5.2. Recommendation	30
REFERENCES	31

LIST OF FIGURES

Figure 1: Different sources of water pollution (Koduru et al., 2019).....	6
Figure 2: Molecular Structure of methylene blue.....	7
Figure 3: Most common waste water treatment methods (Mishra et al., 2021).....	8
Figure 4: Diagrammatic representation of photocatalytic degradation mechanism (Adhikari et al., 2014).....	11
Figure 5: Photocatalytic degradation mechanism ZnO and rare earth element doped-ZnO (R. Kumar & Dosanjh, 2022).....	12
Figure 6: Synthesis of nanostructured materials by bottom-up and top-down approaches.....	13
Figure 7: Diagrammatic representation of solution combustion synthesis method (Abebe et al., 2022).....	14
Figure 8: Schematic illustration of synthesis of ZnO and Eu-doped ZnO.....	16
Figure 9: (a) XRD pattern plots of ZnO, and doped ZnO with 1, 3 and 5% of europium ion; (b) the magnified view of the plots.....	20
Figure 10: (a) DRS-UV-vis analysis spectrum of ZnO and Eu ⁺³ -doped ZnO (b) respective indirect ZnO and EZO nanocomposites Kubelka–Munk function plot, (c) the direct ZnO and EZO nanocomposites Kubelka–Munk function plot.....	21
Figure 11: Photoluminescence spectra plot of ZnO and Eu ⁺³ -doped ZnO (EZO) Nano composite. 1%, 3% and 5% represent the percentage of Eu ⁺³ ions.....	23
Figure 12: FTIR spectra plot of ZnO and Eu ⁺³ -doped ZnO (EZO) Nano composite after calcination of prepared samples.....	24
Figure 13: The percentage effect plots of absorbance versus wavelength (nm) of (a) 1% EZO, (b) 3% EZO, and (c) 5% EZO;.....	26
Figure 14: (a) the plots $CtC0$ versus time (min) of NPs and composites, (b) $lnctc0$ versus time (min) plot of NPs and composites.....	29

LIST OF ACRONYMS

CB	Conduction band
DRS	Differential reflectance spectroscopy
EZO	Europium doped Zinc oxide
FT-IR	Fourier Transforms Infrared
MB	Methylene blue
NPs	Nanoparticles
PL	Photoluminescence
PVA	Polyvinyl alcohol
VB	Valence band
XRD	X-ray diffractometer

ABSTRACT

The doping of rare earth element like europium ions into the ZnO matrix and can considerably enhance photocatalytic performance. Here in this study, Eu^{+3} -doped ZnO (EZO) Nano composite was prepared by using simple solution combustion method. The nanostructured materials that contain different amount of europium ion were synthesized starting from zinc and Europium nitrate as precursor of sol. The disappearance of independent Europium oxide peaks on the XRD pattern of composite and the presence of a low-angle peak shift confirm the successful inclusion of Europium ion within ZnO lattice. The slightly reduction of direct and indirect DRS-UV-vis bandgap energy for EZO nanocomposites relative to ZnO (3.21eV) supports the evidence of Europium ion inclusion in ZnO matrix interpretation. Moreover, the Eu^{+3} -doped ZnO (EZO) Nanocompositewave length shift of photoluminescence spectra and intensity reduction compared to ZnO also confirms the improvement of visible light absorption and the hindrance of electro-holes recombination. Thus, it's possible to deduce that, the Eu^{+3} -doped ZnO (EZO) Nanocomposite has better charge transfer and visible light absorption properties than ZnO nanoparticles (NPs). The Fourier Transform Infrared (FTIR) spectral investigation provides the information about the presence of expected chemical bonding and functional groups attached to Europium ion (Eu^{3+}) doped and undoped zinc oxide (ZnO) nanoparticles. The prepared EZO nanocomposites exhibited advanced photocatalytic activities ($k=0.03 \text{ min}^{-1}$) relative to ZnO ($k=0.02 \text{ min}^{-1}$). The enhanced of photocatalytic degradation of methylene blue dye is attributed to the improved light absorption and charge transfer ability of Eu^{+3} -doped ZnO (EZO) Nanocomposite.

Keywords: Eu^{+3} -doped ZnO nanocomposite, methylene blue, photocatalysis

CHAPTER ONE

1. INTRODUCTION

1.1. Background of Study

Much of industrial pollutants that are found in the environment particularly in water pose critical health risks to human life. Nowadays, the removal of these harmful pollutants, mainly organic dyes, is the critical environmental challenge (Ahmad et al., 2020). Methylene blue (MB) is a widely used synthetic dye in the textile, paper, and pharmaceutical industries. However, its recalcitrant nature makes it difficult to remove by traditional methods, such as adsorption or coagulation (Xia et al., 2020). Recently photocatalysis, which involves the use of semiconductor materials is a promising method to degrade organic contaminants under light irradiation (Balapure et al., 2024). Among several semiconductor photocatalysts, zinc oxide (ZnO) has got significant consideration because of its good photocatalytic performance, harmlessness and chemical stability. ZnO is a wide-bandgap (3.37 eV) semiconductor material that exhibits excellent photocatalytic properties under ultraviolet (UV) light. It has attracted wide attention in this area due to their exceptional structural and functional properties which are applied for potential applications in energy, environmental nanotechnology and photocatalytic degradation of pollutants to change harmful and toxic organic pollutants into harmless products (Kshirsagar et al., 2024). Herein, the photocatalytic process valence band holes and conduction band electrons are produced on the surface of semiconductors when photons from the light source such as UV and visible light interact with catalyst, thus these photon induced holes are further react with H_2O or OH^- , which are attached on the catalytic surfaces to generate hydroxyl radical ($\cdot OH$), and electrons in the conduction band interact with adsorbed O_2 to yield superoxide radical ($\cdot O_2$) (Rong et al., 2022). Despite these advantages ZnO's photocatalytic activity is primarily limited to UV light, which accounts for only a small portion of the sunlight range.

However, ZnO's inadequate visible light absorption limits its photocatalytic efficiency under the irradiation of natural sunlight. In order to overcome this drawback, doping ZnO with rare-earth metal such as europium (Eu^{3+}) have been explored. The doping of Eu^{3+} ions into ZnO can improve its light absorption, particularly in the visible region, and enhance its photocatalytic properties (Al Rifai & Kulnitskiy, 2013; Applications, 2022; Armelao et al., 2008). This limitation can be solved by modifying the surface of ZnO by introducing dopants that extend its visible light absorption. Rare-earth metal ions like Eu^{3+} are ideal candidates due to their

exceptional optical belongings, containing good fluorescence performance and the ability to sensitize the material for enhanced photocatalytic activity. The inclusion of Eu^{3+} ions in the ZnO lattice enhances its photocatalytic activity by facilitating the formation of more photon induced electron-hole pairs under the irradiation of visible light, improving the overall material's catalytic performance. The incorporation of dopants within host materials results in the improvement of surface area and generates lattice defects and modifies bandgap energy of the host ZnO (M. Kumar et al., 2021). Most lanthanides elements ions show high luminescent intensity due to their 4f- intra shell shifts can produce bright luminescence spectrum. From those elements, europium ion (Eu^{3+}) shows a robust release because of the 4f- 4f transition of electrons (Gemechu et al, 2022).

Numerous ZnO-based catalyst implementation possibilities improvements through doping procedures were well studied and reported. Al Rifai et al. synthesized Europium-doped ZnO by a chemical vapor deposition method. The successful preparation of the material was confirmed by the XRD, SEM-EDX, and more photoluminescence analysis (Al Rifai & Kulnitskiy, 2013). Kumar et al. synthesized Europium Eu^{3+} -doped ZnO nanomaterial via facial co-precipitation method. In this study the improvement in photonic properties of doped material was explained through invoking the presence of Eu^{3+} electron in the band gap of ZnO (M. Kumar et al., 2021). El Jouad et al. synthesized europium doped ZnO thin films using a spray pyrolysis method for optoelectronics applications. Besides, the inclusion of europium ion in the ZnO lattice was also confirmed from the slight angle peak shift compared to the single ZnO (El Jouad et al., 2020).

The porosity nature of materials improves surface area which helps for good collaboration of catalysts with pollutants. Solution incineration synthesis method has an efficient approach for preparing porous materials (Perego et al., 2013). Though, it produces high amounts of heat and facilitates the aggregation of NPs because of high surface energy (Saxena et al., 2017). Accordingly, become stable agent such as polyvinylpyrrolidone (PVP) and polyvinyl alcohol (PVA) should be used. The polymer PVA is widely used as a surfactant due to its good mechanical characteristic and non-toxicity. Moreover, it can participate in exothermic reactions and provide heat needed during combustion synthesis (Abebe et al., 2022). Mohammed et al. synthesized a porous Co-doped ZnO/Ag heterostructure using a PVA

capping agent. In addition, the PVA polymer used as fuel that helps the combustion process and generates a wormhole-like porous material (Mohammed et al., 2025).

Based on the over head evidences, the situation is fascinating to synthesize Eu^{+3} -doped ZnO (EZO) Nanocomposite through solution combustion approach for overcoming ZnO's drawback and advancing this one Photocatalytic efficiency. Besides, the Eu^{+3} -doped ZnO (EZO) Nanocomposite, which is prepared through solution combustion approach has not yet been reported for degradation of methylene blue. The inclusion of europium in the ZnO lattice was found to boost the photocatalytic degradation application. This degradation efficiency enhancement is connected with the photonic property improvement due to the insertion Eu^{+3} within ZnO matrix.

1.2. Statement of the Problem

The main sources of water pollution and the intensification in fabrication of synthetic dyes are attributed on the way to their high consumption in others industries, typically the textile industries are the primary cause for water pollution by methylene blue dye. Methylene blue dye is stable against water, temperature and light, as a result it cannot be frequently removed during the traditional wastewater handling methods (Ahmad et al., 2020), because this dye has continuing to exist in our environment. As MB dye present in food source and drinking water, it can seriously damage a person's physical and nervous system. Therefore, the elimination of this pollutant has become the serious issue currently (Alanazi et al., 2021).

Essentially, there are a lot of traditional wastewater treatment methods that work based on chemical and physical principles, however due to the intricate technique and processes involved, the prerequisite of expensive equipment and chemicals and secondary pollutant generation their practical advantages is often constrained and cost of existing removal methods (Cheng et al., 2020). Currently, heterogeneous photocatalytic oxidation through ZnO catalyst is an advisable method of MB removal. But, the main problems of using ZnO as photocatalysts photon induce electrons-holes recombination (EHR) and are lack of harvesting visible light. As a result, to solve these drawbacks of ZnO, doping with transition metals was used in the previous works (Mengistu et al., 2023). These problems are expected to be overcome by developing Eu^{+3} -doped ZnO (EZO) nanocomposite material via a solution combustion synthesis method.

1.3.Objective of the Study

1.3.1. General objective

The general objective of this study is to synthesize and characterize Eu⁺³-doped ZnO (EZO) Nanocomposite for Photocatalytic degradation of methylene blue dye.

1.3.2. Specific objective

- To synthesize ZnO NPs
- To synthesize Eu⁺³-doped ZnO (EZO)Nanocomposite
- To characterize the synthesized NPs and composites using different systematic techniques such as XRD, DRS-UV-vis, PL and FTIR.
- To investigate those methylene blue dye degradation capabilities of synthesized ZnO NPs and Eu⁺³-doped ZnO (EZO)Nanocomposite.

1.4.Significance of the Study

This study showed a low-cost, environmentally sustainable solution for degrading methylene blue dye using Eu⁺³-doped ZnO (EZO) Nanocomposite. Moreover, Eu⁺³-doped ZnO (EZO)Nanocomposite catalytic performance was enhanced by using solution combustion method to produce porous material, providing efficient pollutant degradation. From the result of this study, all communities, industries, the scientific community, and future researchers will be benefited. This research opens the chance for further research on the development of advanced methods for the water purification.

1.5.Scope of the Study

The scope of this study was restricted to the fabrication in connection with ZnO, and Eu⁺³-doped ZnO (EZO) Nanocomposite, using a portion solution combustion techniques; the characterization of as prepared nanoparticles and composites utilizing XRD, UV-Vis- DRS, PL, and FTIR analytical technique. UV-Vis spectroscopy also applied for the investigation photocatalytic activity of as-synthesized nanomaterial's on synthetic methylene blue dye.

CHAPTER TWO

2.LITERATURE REVIEW

2.1. The pollution of Water

Water pollution is occurred commonly associated with the discharge of industrial effluents which consist extensive amount of dyes, aromatic, heavy metal ions and the decomposed product of herbicides and pesticide (S. Naseer et al., 2022). The pollution of water by toxic dyes is a considerable environmental problematic throughout the world recently. A lot of industries like textile, leather, printing, paper, etc. discharge a large amount of hazardous pollutant to water bodies(Mondal et al., 2019). The discharge of toxic dyes to water parts usually results in the unwanted coloring of the water surface, which commonly resists sunlight from passing the water surface and used in the photochemical and biological functions important for aquatic life (Lam et al., 2012). Rafi et al (2021) reported that, based on the World Bank report, around 17-20% of contamination of water came from textile industries and treatment; therefore, textile industries represents the pollution of water problem internationally because of accidental discharge of polluted water in to the water bodies, which shows a major influence on the cleanliness of water resources.

The pollution of water bodies due to water-borne pathogen and also related diseases; are a serious problem that concern around the world. Pollution of water by pathogens is a severe problem for all form of water bodies is critical issue(Magana-Arachchi& Wanigatunge, 2020). Besides, rivers have been polluted by incomplete treated and/or untreated discharge from petrochemicals, rolling steel mills oil spills, and pesticides pollutant. In addition, it should be known that the comparative high stability synthetic dyes results health and environmental difficulties because of their carcinogenic poisonous and mutagenic properties (Sarkar Phyllis et al., 2022).



Figure 1: Different sources of water pollution(Koduru et al., 2019)

2.1.1. Properties of methylene blue (MB) dye

The organic dye compounds have been released from different industries as effluents are the main cause of pollution and eutrophication in aquatic environment. Synthetic dyes are commonly applied in large amounts in the textile industries, which are physically and chemically stable compounds and hazardous to our environment (Adeel et al., 2021). From synthetic organic dyes; methylene blue (MB) is a famous cationic and thiazine organic dye with chemical formula-($C_{16}H_{18}ClN_3S$), and having λ_{max} of 664 nm, is a solid dark blue powder at room temperature and forms blue solution after complete dissolution in water; soluble in water, ethanol, methanol, acetone and ethyl acetate (Hamad & Idrus, 2022). MB is carcinogenic dye that has been prepared and used in several industries for different purposes like dyeing of cotton, coloring of paper, wool and fabrics hair, and indicator of redox reaction (Riggert et al., 2001). It induces a grave problem to human health such as damaging nervous system and eyes. Besides, it results nausea, breathing difficulty, diarrhea, and vomiting. Thus, it is important to eradicate this toxic pollutant from water bodies. In Photocatalytic degradation of Methylene blue study, UV-Vis analysis is very essential to analyze the change in absorbance curve due to the presence of catalyst and to compare the efficiency of catalyst

by calculating the degradation efficiency and reaction rate constant (Akhmal Saadon et al., 2016).

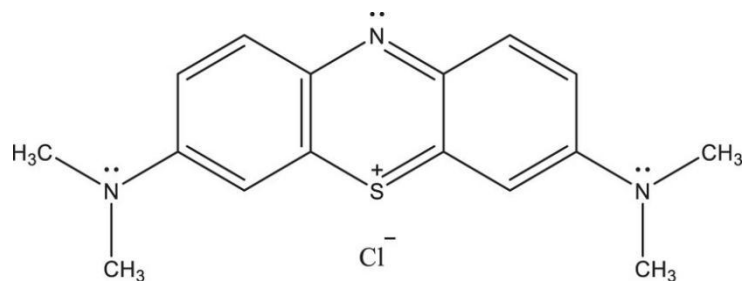


Figure 2: Molecular Structure of methylene blue

2.1.2. Methods used to remove MB from water

Usually, the treatment waste water follows four main stages, such as preliminary, primary, secondary and tertiary processes. In detailed, preliminary processes used for the elimination of large substances like grits, plastics, papers, wood etc fundamental remediation includes skimming to eradicate frothy solids and flotation and sedimentation to eliminate settleable impurities. Then, secondary treatment includes the fail of dissolved microbial and colloidal equipment (Hamad & Idrus, 2022). Tertiary treatments involves an advanced method especially, applied for methylene blue removal, which includes biological agent (aerobic, anaerobic, anoxic or facultative), chemical agents (chemical precipitation, ozonation, ion exchange, photocatalysis and ultrasound) and physical (sedimentation, coagulation, membrane filtration, flocculation filtration, and adsorption) (Collivignarelli et al., 2019). Though, previous studies reported several techniques that used waste water treatment application as demonstrated in Fig.3. Whereas, photocatalysis provides an extensive variety of advantages due to its simple set up, cost effectiveness, lower energy consumption, high pollutant degradation efficiency without the generation of hazardous by-products (Sarkar Phyllis et al., 2022).

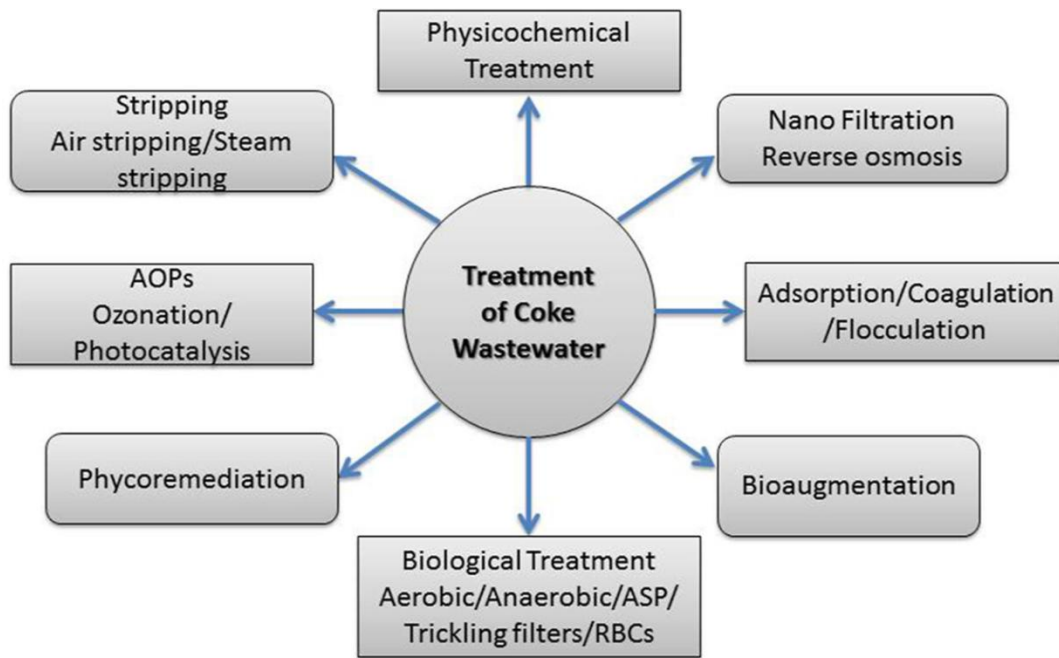


Figure 3: Most common waste water treatment methods(Mishra et al., 2021)

2.2. Introduction to Nanotechnology and Nanomaterial's

Nanotechnology refers to a technology of propose manufacture and application of nanostructure materials, as well as also an crucial empathetic of physical property and phenomenon of Nanomaterial's(Köhler & Fritzsche, 2008). It is a fast developing field in science and technology for the application of fabricating material in nanoscale. Many companies in the world are presently trying to use nanotechnology to create their inventions more productivein terms of structure, functioning, and designing of materials (Khin et al., 2012). It has allowed the civilization of all industrial domain, starting from small-scale production and processing units in the medicine ,agriculture and food industries to larger-scale production units (Xia et al., 2020).

Nanomaterial's, compare to bulk substances, have the scales ranging from individual atoms or molecules to submicron scope at least in one dimension (Policy, 2015). They have unique chemical and physical properties that able to be used for different purpose. The important of nanotechnology was firstly described by Feynman, during the science lecture allowed “There is plenty of room at the bottom” at the annual meeting of the American Physical Society in 1959 (Reed et al., 2014). A lot of discoveries and innovation in the manufacturing of nano objects have been established. The fabrication of novel materials, processes and phenomena at the nanoscale, and also the improvement of new experimental and theoretical techniques for research work give many new opportunities for the establishment of innovative nanostructures

materials. Nanostructured materials can be fabricated with exception nanostructures and properties. This field has predictable to open new era in science and technology.

2.3. Nanoparticles (NPs)

Nanoparticles (NPs) are a types of nanomaterial's that have the size 1-100nm in diameter in all dimension(Vasyliiev et al., 2020).It is hard to observe nanoparticles by standard optical microscopes, needing the use of laser microscopes or electron microscopes.They have an exceptional size-dependent feature known as high 'aspect ratio', refers to the high surface area to volume ratio..Particle size with aspect ratio has indirect relationships; when small size descends the aspect ratio will ascends. That means they have a high surface area than volume. The enlarged outside Local of the smaller nanoparticles will increases their reactivity (Khin et al., 2012)).

2.3.1. Zinc oxide (ZnO) nanoparticles

Zinc oxide (ZnO) is an extended band gap II-VI semiconductor known used for high electron mobility, optical transparency, and room-temperature luminescence. It has a white color appearance, is usually known as zinc white or zincate, as well as it is insoluble in water and alcohol, however it soluble in acids like hydrochloric acid. Due to ZnO turns yellow when heated and white when cooled, it is thermochromic in its crystalline form (Puspitasari et al., 2018). It has three crystal forms such as hexagonal wurtzite, the cubic zinc blende, and the cubic rock salt. The most known structure is wurtzite, which shows the high stability under normal conditions. Each individual anions in wurtzite hexagonal structure has a pattern parameter of $a = 0.3296$ nm and $c = 0.520$ nm, with space group P63mc and point group C6v4, is surrounded by four Cations in the corners of the tetrahedron, displaying tetrahedral coordination and sp^3 covalent bonding (Liu et al., 2019).

ZnO provides a lot of attractive features, including high electron mobility, non-toxicity, biocompatibility, outstanding transparency, high photocatalytic activity, high stability and strong room-temperature luminescence (Abebe & Ananda Murthy, 2022). UV lasers, Solar cells, optoelectronics, laser diodes, transparent conductive contacts, beam emitter diodes, gas probes, surface acoustic wave devices, and piezoelectric devices and thin-film transistors are all use ZnO nanoparticles in some way. ZnO nanomaterial's have been employed in a multiple implementations such as cosmetics, electronics, optics, and photocatalytic degradation of organic dyes(Klingshirn et al., 2010). Compared to other semiconductor metal oxides, ZnO has a greatest degree of lattice defects, allowing it an excellent photocatalysts material.

Surface area, Phase purity, crystallite size, synthesis procedures and dopants kind are all key factor in determining photocatalytic efficiency(Yang et al., 2013).

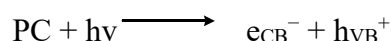
2.4. Photocatalysis

The word photocatalysis combines the terms “phos,” which means light, and “katatalyo, ” which means to decompose. Generally, photocatalysis describes alteration in the speed of a chemical process caused by visible light or ultraviolet light in the occurrence of a material that captures light and participates in chemical change of reactants. A material that captures visible or ultraviolet light and produces reactive species when excited is called a photocatalysts (Chong et al., 2024).

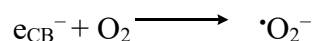
The photocatalytic reactions can occur in either homogeneous systems or heterogeneous; but, heterogeneous photocatalysts have obtained a lot more interest due to its ability uses in several fields, including the generation of energy and cleanup of environments. Moreover, heterogeneous photocatalysts are simply separated from a reaction mixture, allowing them appropriate for application in additional reactions(Perego et al., 2013).

2.4.1. Mechanism of photocatalytic degradation

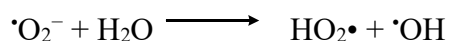
The photocatalytic degradation of pollutant mostly involve a few steps starting from adsorption-desorption, electron-hole pair production and chemical reaction. The overall mechanism of photocatalytic degradation of organic molecules best described in the equations below (Thennarasu & Sivasamy, 2013). Once the photocatalysts is irradiated with light energy with required band gap energy of PC, then electrons are jump from the valence band (VB) to the conduction band (CB) nm it the concurrent formation of holes (h^+) in the VB:



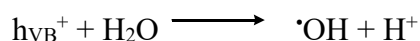
The electrons produced by irradiation could be easily trapped by O_2 molecule which is absorbed on the photocatalyst surface to give superoxide radicals ($\cdot O_2^-$):



Thus, $\cdot O_2^-$ could react with H_2O molecule to generate hydroperoxyl radical ($HO_2\cdot$) and hydroxyl radical ($\cdot OH$), those are strong oxidizing agents to degrade the organic molecule:



At the same time, the photon induced holes could be trapped by surface hydroxyl groups (or H₂O) to give hydroxyl radicals ([•]OH):



Lastly, the organic molecules will be decomposed to give carbon dioxide and water as follows:

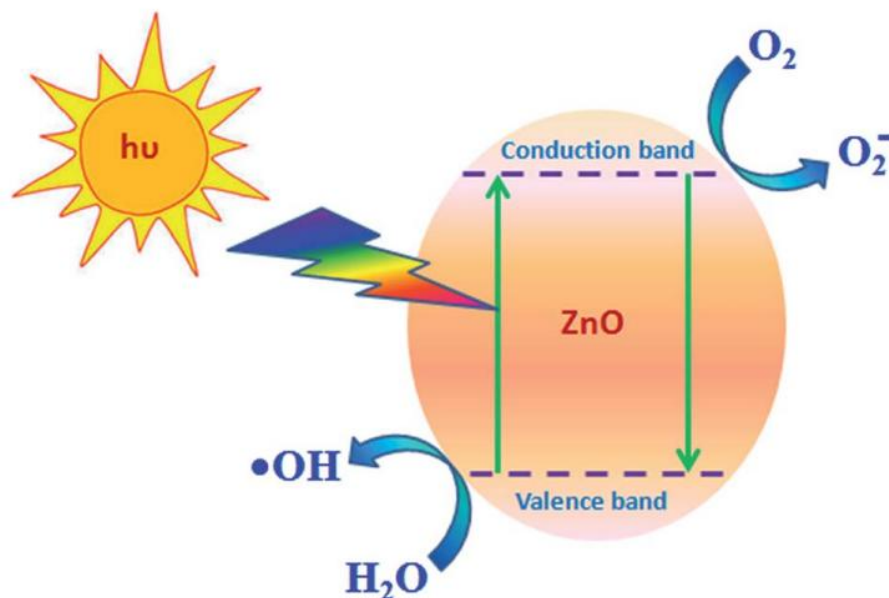
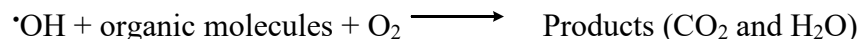


Figure 4: Diagrammatic representation of photocatalytic degradation mechanism(Adhikari et al., 2014)

2.5. Doping

Nowadays, nanotechnology has proceeded to improvement in fabricating nanomaterials for waste water treatment through doping, can advanced the optoelectronic properties of metal oxide semiconductors (Molavi et al., 2024). Doping of transition metals can tune optical properties of host materials and absorption of visible light(Abebe & Ananda Murthy, 2022). Doping ZnO with rare earth elements like Europium can significantly improve its photocatalytic properties through encouraging charge separation and resisting electron-hole recombination. Europium (Eu⁺³) ions, due to their luminescent properties can improve the band structure of ZnO. Furthermore, Europium doping assists for inhibiting the recombination of photon induced electron-holes pairs; which helps to increasing a lifetime of electron-hole pairs. Then, this separation of charges used to facilitate more effective electron transfer to the dye molecules

leading to a more efficient degradation process (El Jouad et al., 2020). Besides, it is used for bandgap energy modification; Europium ions also play a crucial role in modifying the ZnO bandgap, making it more appropriate for photocatalysis beneath visible light which is more prominent than UV light. This helps for better utilization of solar energy in photocatalytic degradation applications (Armelaio et al., 2008).

When Eu^{+3} ions are inserted into ZnO lattice, they may occupy Zn^{+2} sites within the ZnO matrix. The inclusion of Eu^{+3} ions introduces new energy levels within the bandgap of ZnO, which can change both the optical and electronic characteristics of the material. Eu^{+3} naturally assist to photoluminescence spectrum in the red-orange region associated with $5\text{D}^0 \rightarrow 7\text{F}^2$ electron transitions, while Eu^{2+} may give to blue or green emissions; the emission properties dependent on the concentration of dopant, the local environment of the Eu ions, and the synthesis conditions (Al Rifai & Kulnitskiy, 2013). The main effect of doping with Eu is the improvement of the luminescent properties. Europium doping advances the photoluminescence characteristics, leading the material to release light at specific wavelengths. These fascinating luminescent properties are valuable for several applications in optoelectronics, like in phosphors for displays or light-emitting diodes (LEDs). Moreover, doping can affect the morphology and crystalline of ZnO nanoparticles (Applications, 2022).

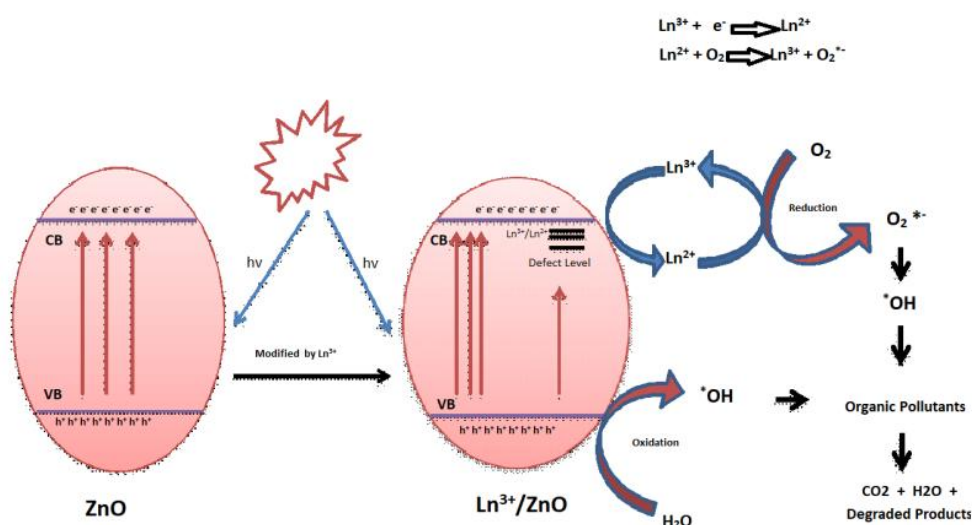


Figure 5: Photocatalytic degradation mechanism ZnO and rare earth element doped-ZnO (R. Kumar & Dosanjh, 2022)

2.6. Synthesis methods

The synthesis of nanostructured materials involves several approaches were applied to achieve high catalytic efficiency and structural integrity (Iqbal et al., 2012). The synthesis methods can be top down or bottom up approaches, as illustrated in Fig. 6.

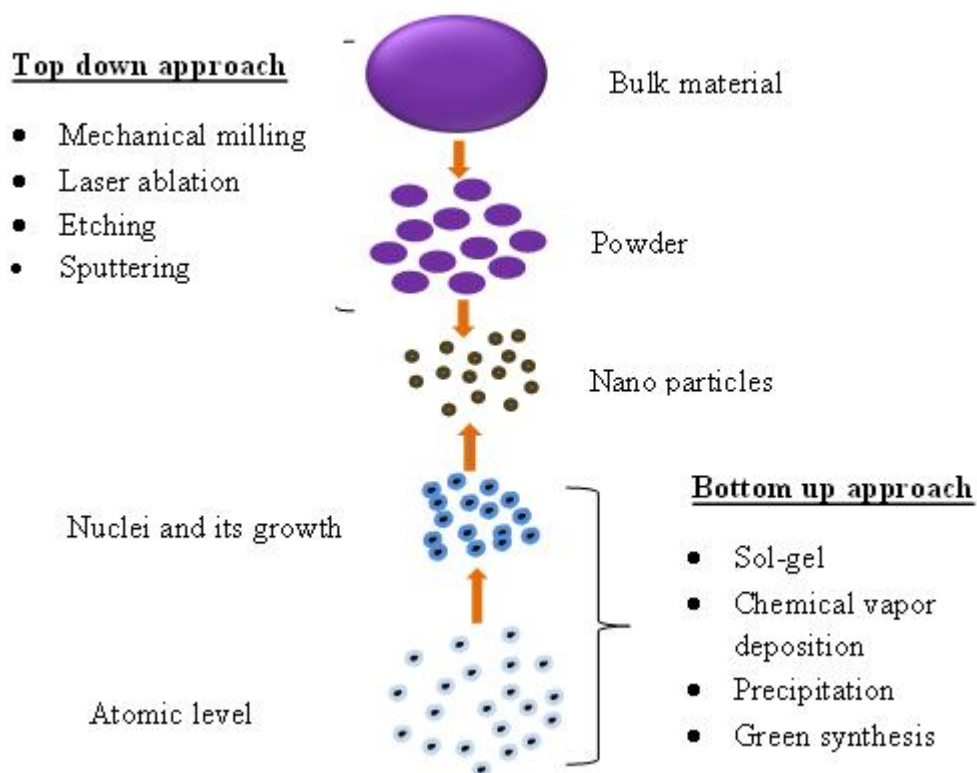


Figure 6: Synthesis of nanostructured materials by bottom-up and top-down approaches

a) Solution combustion synthesis approach

The synthesis method which is solution combustion synthesis is a fast, simple, time/energy effective process; it works based on propellant chemistry and the stoichiometric ratio fuel to oxidant (precursor). In this method the reaction between organic fuel (reducer) and metal precursors (oxidizer) results exothermic reaction, which produce intense evolution of gases (Chen et al., 2021), has a good compensation as a liquid phase chemical method. The emission of NO_2 and CO_2 gases allows self-sustained and auto-catalytic combustion reaction between intermediate phases. Solution combustion reaction is conducted when the reaction temperature surpasses the ignition temperature of redox (oxidant and fuel) solution (Siddique et al., 2022). The reaction carried out at high speed and nanomaterial is created with uniform porous structure (Nersisyan et al., 2017). The main stages of this synthesis method are formation of colloidal solution of oxidant and fuel (reducer), transformation of sol to gel and

combustion of gel to produce metal oxide nanoparticles (Yin et al., 2023). Fig. 7, Summarizes the steps involved in solution combustion synthesis method.

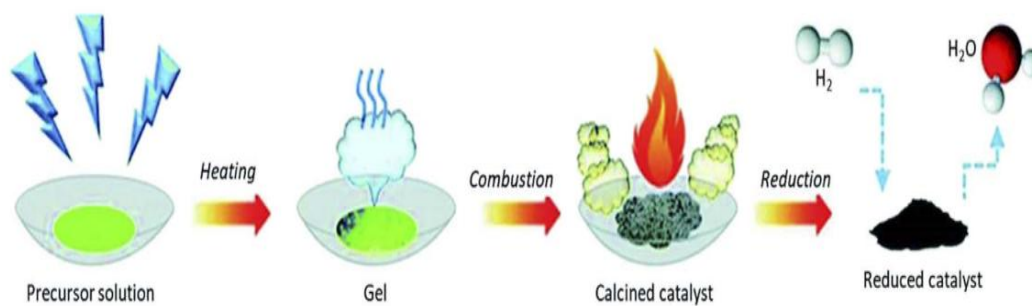


Figure 7: Diagrammatic representation of solution combustion synthesis method (Abebe et al., 2022)

CHAPTER THREE

3. MATERIALS AND METHODS

3.1. Experimental Site

This research was carried out in Adama Science and Technology University (ASTU); Applied chemistry, Materials Science and Engineering and Applied Physics laboratories. Moreover, chemicals were purchased from a well-known market. The synthesis of materials was conducted at Adama Science and Technology University in applied Chemistry laboratory. XRD, photocatalytic degradation of MB and UV-Vis DRS spectroscopy analysis was performed in ASTU Materials Science and Engineering laboratory. Photoluminescence analysis was carried out in ASTU applied physics laboratory. In addition, FT-IR was carried out at Addis Ababa Science and Technology University at industrial chemistry department laboratory.

3.2. Chemicals and Reagents

The chemicals that used in this study are; Analytical grade chemicals such as Zinc nitrate hexa-hydrate ($\text{Zn}(\text{NO}_3)_2 \cdot 6\text{H}_2\text{O}$, 99.5%, Sigma Aldrich, Germany), Europium nitrate ($\text{Eu}(\text{NO}_3)_3$, 99.5%, Sigma Aldrich, Germany), Polyvinyl alcohol (PVA, Thermo Fisher Scientific India Pvt) and Reagents such as ethanol (97%), Ammonium hydroxide (NH_4OH), distilled water and HCl and methylene blue dye (82%, Sigma Aldrich) for the investigation of photocatalytic activities of the as-synthesized catalysts.

3.3. Equipment and Instruments

The powder X -ray diffractometer (XRD) is used for the crystallinity analysis of the as-synthesized powders. To study the optical properties of samples DRS-UV-Vis, and PL spectrophotometer was used. FTIR also used to study the functional bonding and chemical bonding between metal and oxygen, and other functional groups that found in synthesized samples.

3.4. Synthesis of Photocatalysts

Synthesizing nanomaterials using simple approaches like combustion reduces time and cost and makes it easier for scaling up production. Herein, the solution combustion chemical strategies(Abebe, et al., 2023)with a certain modifications was used to synthesize photocatalysts. To synthesize single ZnO NPs, 0.5g of PVA was dissolved in 50 mL of distilled water and stirred continuously for about 15 minutes at 70°C. After the complete dissolution of PVA polymer, the aqueous solution was cooled down to room temperature. The

zinc precursor solution was prepared by adding $\text{Zn}(\text{NO}_3)_2 \cdot 6\text{H}_2\text{O}$ salt in the cooled PVA surfactant solution along with the continuous stirring on a magnetic stirrer at about 65°C . After the full liquefaction of suspension, the final sol was permitted to cool to room temperature. Then, the evaporation was takes placed on hot plate at 100°C to form a gel. Additional heating the gel to the zinc salt precursor-PVA polymer ignition temperature of $150\text{-}240^\circ\text{C}$, the combustion/self-propagation process occurred. The final combusted material was crushed and calcined in the muffle furnace at 450°C for about 1hr. The calcination helps in removal of different impurities in order to produce a stable ZnO nanocrystal.

Likewise, with varying concentrations of Zinc and Europium precursors, a series of 1%, 3%, and 5% Eu^{+3} -doped ZnO nanostructured materials are also synthesized following the same solution combustion approach. In detailed, 0.5 g of PVA was dissolved in 50 mL of water and cooled to room temperature. Then, three samples with various zinc nitrate and Europium nitrate salt precursor percentages were synthesized by liquefaction in a pre-dissolved and cooled PVA polymer solution. The precursor's percentages used to synthesize catalysts are 99, 97 and 95%, for zinc and equal 1%, 3% and 5% percentages for europium nitrate salt. The prepared samples were then coded as 1%, 3%, and 5%, respectively. When the synthesis was carried out, the mixtures were dissolved at 70°C to form a sol; the water was dehydrated at 100°C to form a gel and finally combusted in the temperature range of $150\text{-}240^\circ\text{C}$ and calcined at 450°C for 1 hr. The diagrammatic illustration of the synthesis procedure that shows PVA polymer liquefaction, mixing of the precursors in PVA aqueous solution to form a sol, drying to form gel, and finally calcining to obtain stable nanomaterials was shown in Fig. 8.

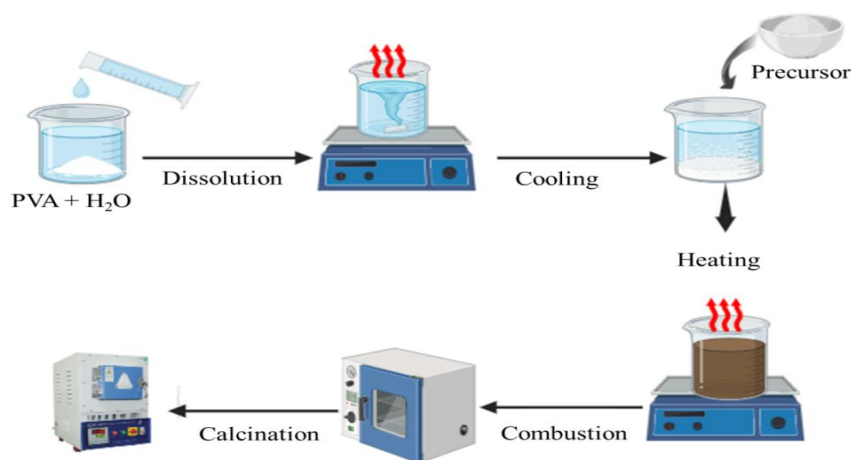


Figure 8: Schematic illustration of synthesis of ZnO and Eu-doped ZnO

3.5. Characterization of as Synthesized Photocatalysts

The solid structure and size of the nanomaterials influenced by several factors including precursor salts, surfactant additives, temperature and reactant concentrations. To progress consistent synthesis of nanomaterials, characterization is found to be important.

Characterization deals with the study of structure, composition and properties of prepared samples (Mudalige et al., 2019).

3.5.1. X-Ray diffraction (XRD)

The structural characteristics of synthesized sample was investigated by the X-ray diffractometer (XRD-7000, SHIMADZU Corporation, Japan) using Cu-K α radiation ($\lambda = 0.15404$ nm) at scan rate of 3°/min. The XRD data was recorded in terms of peaks intensity and 2θ values from 10° to 80° and those data was plotted using origin software. The miller indices of diffraction peaks were indexed according to their corresponding JCPDS files; the diffracted X-rays were then being detected, processed, and counted. Besides, the average crystalline size was calculated from XRD spectra by using Debye-Scherrer equation (Domingues et al., 2024).

$$D = \frac{K\lambda}{\beta \cos\theta} = \frac{0.9 \times 0.15406}{FWHM \cos\theta} \quad (6)$$

Where, D = particle size of the crystal; K = Scherrer constant (usually 0.9); λ = wavelength of X-Ray source, Cu K α radiation (1.5406 Å); β = full width at half-maximum (FWHM) of the diffraction peak in radian; θ = Bragg's diffraction angle

3.5.2. UV-Vis DRS

The band gap of the prepared materials estimated utilizing UV-Vis diffuse reflectance spectrophotometric technique, which give the information about the optical absorption efficiency of as-synthesized nanomaterials materials (Ray et al., 2022). The optical property of samples was investigated with the ultraviolet-visible disperse reflectivity spectroscopic technique (Cary 100 UV-Vis, Agilent Technologies). The solid samples were placed in the sample holder of the DRS instrument, then the reflectance spectrum were collected and the band gap energy of nanomaterials was estimated with help of Kubelka-Munk function plot (Joy et al., 2024).

3.5.3. Photoluminescence (PL)

The emitted light's wavelength of prepared nanomaterials was investigated under optical excitation by a photoluminescence instrument (Cary Eclipse, Agilent Technologies), which gives information about the emission wavelength shift and the reduction of electron holes

recombination (EHR). Lastly, the data was plotted and interpreted in relative to the material's properties and applications (Albert manoharan et al., 2018).

3.5.4. Fourier transform infrared spectroscopy (FT-IR)

The chemical bonding and functional groups which present in fabricated nanomaterials whereconducted by Fourier Transform Infrared spectrometer (FTIR-6600typeA, Jasco). The sample preparation was proceed by mixing small amount of sample with potassium bromide, squeezing it to make a pellet, and putting it on a specimen holder, thus the data was recorded from 400-4000 cm^{-1} (Thennarasu & Sivasamy, 2013).

3.6. Photocatalytic degradation of Methylene Blue Studies

According to the method of recent trails (D. Singh et al., 2024), the photocatalytic efficiency of prepared samples was tested by the degradation of methylene blue dye . The experiments were carried out by taking 100 mL of methylene blue dye in an aqueous solution (10 mg/L) with a required amount of the prepared photocatalysts. In detailed, before illumination, the reaction mixture was stirred continuously in the dark condition for around 30 minutes to formthe adsorption/desorption equilibrium of the dye on the photocatalysts. After 30 minutes, depending on the UV-Vis DRS characterization results of the nanomaterials, a 150 W tungsten halogen lamp as the light source was used. The samples were irradiated directly by focusing light into the reaction mixture at a standard distance from the reactor. Magnetic stirring was applied to continuously mix the solution. The temperature of the overall reactor controlled by a water circulation. With ten (10) minutes interval approximately 4 mL MB solution was withdrawn, the solution was centrifuged to remove the photocatalyst from the sample. The methylene blue dye concentration was measured by UV-vis spectrophotometer (UV-3600 Plus series) at the absorption maximumu wavelength at $\lambda_{\text{max}}= 664 \text{ nm}$ and reaction dynamics study also understood from the reaction kinetic equation.In this study the mathematical treatment of the reactions was simplified by Pseudo-first-order kinetics equation. This equation enhances data analysis and helps for determination of reaction rate constant.

3.6.1. Effect of some operational parameter

Effects of few operational parameters which are photocatalyst dosage (10, 20 and 30 mg) and percentages (1%, 3% and 5%) of dopants were investigated for the selected catalyst in order to optimize the degradation performance.

CHAPTER FOUR

RESULT AND DISCUSSION

4.1. X-Ray diffraction (XRD) Pattern Analysis

The purity of phases and crystal structure of prepared single and EZO nanomaterials were investigated using XRD technique. The X-Ray diffraction pattern peaks of single ZnO, and Eu_2O_3 match with the hexagonal wurtzite (JCPDS# 00-036-1451) and monoclinic (JCPDS# 00-043-1008) structures, respectively. The detected diffraction patterns for ZnO NPs occurred at 31.5° , 34° , 36° , 47.5° , 56.5° , 63° , and 67° 2θ values, as corresponding to (100), (002), (101), (102), (110), (103), and (112) lattice planes, correspondingly as depicted in (Fig. 9a). At all percentages of dopant concentration (1, 3, and 5%), the Eu^{+3} -doped ZnO (EZO) Nanocomposite XRD peaks revealed only a scattering patterns similar to the wurtzite structure of ZnO, confirms the fascinating incorporation of Eu^{+3} rare earth metal ion within the ZnO lattice. Besides, there are no scattering peaks of Eu_2O_3 observed in the X-Ray diffraction patterns of Eu^{+3} -doped ZnO (EZO) Nanocomposite. All the diffraction patterns of doped materials are shifted to lower 2θ value, this is due to the increase in lattice strain by doping of Eu^{+3} ions which have greater ionic size (0.95 \AA) than ionic radius of ZnO (0.74 \AA) in tetrahedral coordination (Al Rifai & Kulnitskiy, 2013). According to the above facts, it's reasonable to deduce that the solubility of europium ion in the ZnO matrix is much better. Therefore, the nonappearance of the Eu_2O_3 crystal phase is also described to be associated its high dispersion and minimum density distribution (Wang et al., 2022).

The average crystalline size of ZnO NPs and Eu^{+3} -doped ZnO (EZO) Nanocomposite was calculated using the Debye-Scherrer equation. $(K\lambda/\beta \cos\theta = (0.9 \times 0.15406)/(\text{FWHM} \cos\theta)$ where, D denotes the crystal average particle size; k denotes the Scherrer constant, which is taken as 0.9 for this study; λ represents a wavelength of X-ray source at Cu $K\alpha$ radiation (0.15406 nm); β denotes diffraction peaks full width at mid-peak; and θ is Bragg's angle of diffraction.

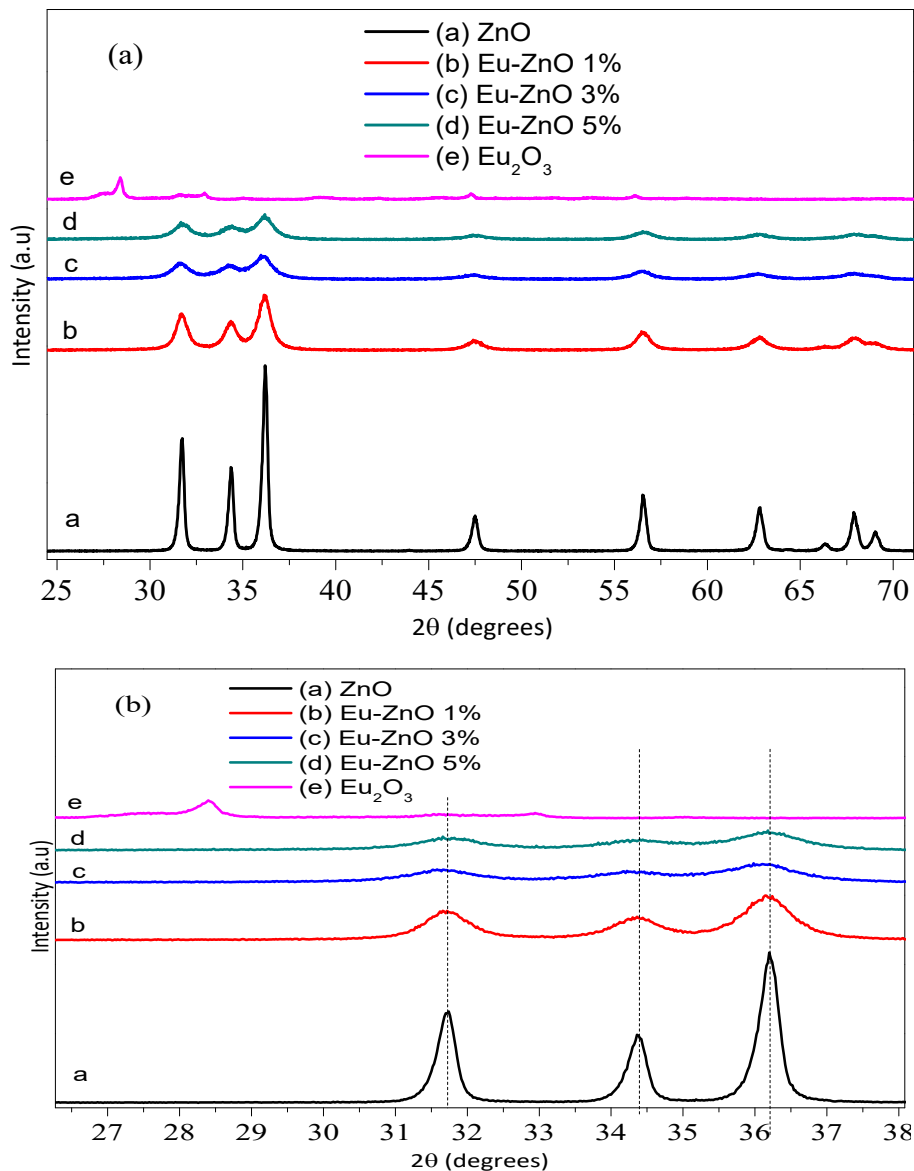


Figure 9:(a) XRD pattern plots of ZnO, and doped ZnO with 1, 3 and 5% of europium ion; (b) the magnified view of the plots.

4.2. UV Visible-DR-Sanalysis

The DRS-UV-Vis spectra analyses were used for the investigation of optical properties of the prepared ZnO and different percentage of Eu^{+3} -doped ZnO (EZO) Nanocomposite is presented in Fig. 10 (a-c). As shown Fig.10a; the strong reflection band at about 380-400nm is due to the ZnO's near band vergedistinctive reflection. The reflection bands at higher wavelength are also reported to be $4f \rightarrow 4f$ electron transition, confirming the inclusion of europium ion with in ZnO lattice(El Jouad et al., 2020).

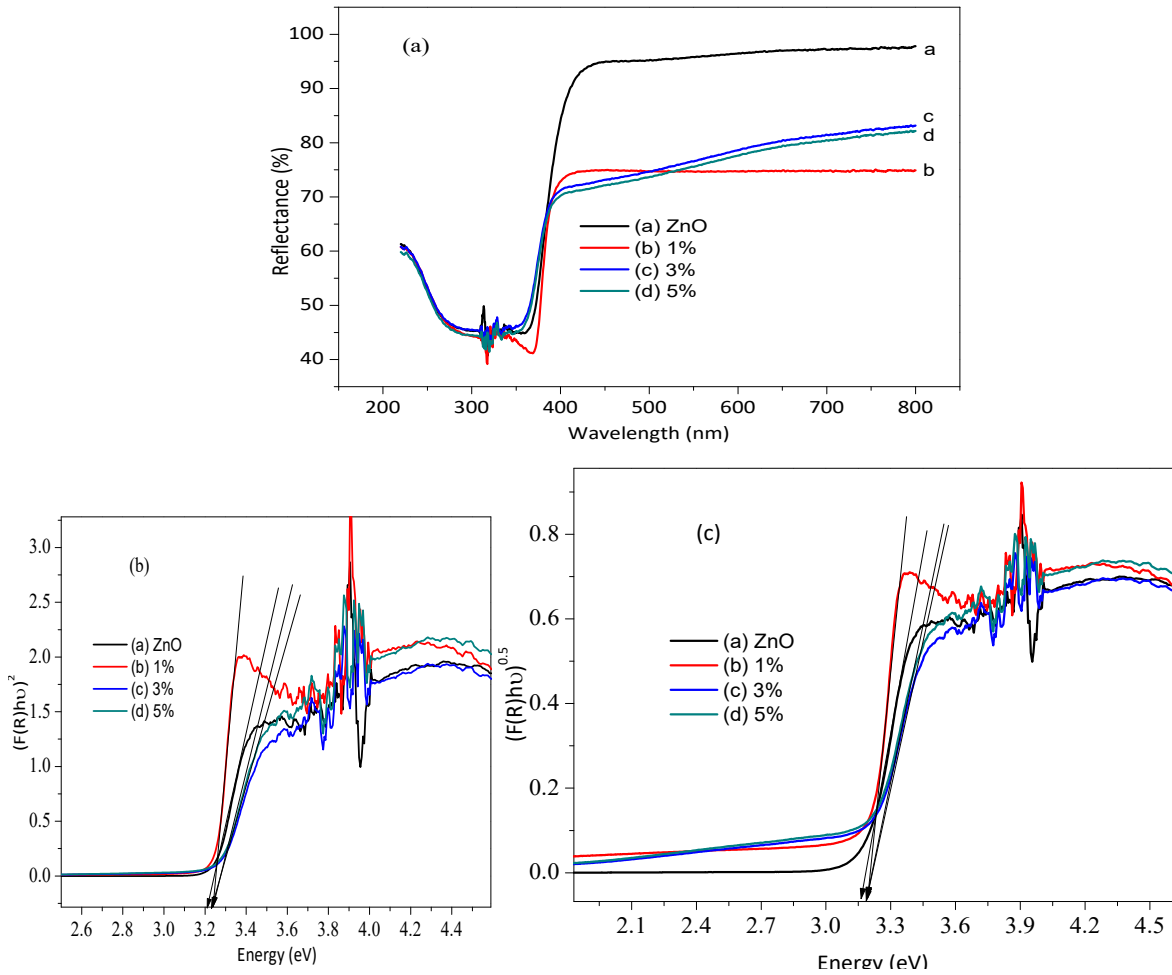


Figure 10: (a) DRS-UV-vis analysis spectrum of ZnO and Eu^{+3} -doped ZnO (b) respective indirect ZnO and EZO Nanocomposite Kubelka–Munk function plot, (c) the direct ZnO and EZO Nanocomposite Kubelka–Munk function plot.

The semiconductor materials are classified in to direct and indirect based on the precious stone momentum (k -factor) values. When the k -factor value in the maximum valence band (VB) and minimum conduction band (CB) is equal the materials said to be direct semiconductor materials. Then, the electron at higher level pairs up and directly emits the absorbed light. Conversely, in the indirect materials, the k -factor value turn out to be different, thus the excited electron gets relaxation time. Throughout this relaxation time the holes react with water and also electron interact with oxygen to produce the highly reactive species, hydroxyl radicals ($\cdot\text{OH}$). In the Eu^{+3} -doped ZnO nanocomposites, the incorporation of europium in the ZnO matrix forms defects within the VB and CB, which helps electron relaxation. Therefore, the direct and indirect bandgap energy of synthesized Eu^{+3} -doped ZnO was considered and

calculated based on the Kubelka–Munk function plot (Fig. 10 a-b). The estimated direct band gap energy for Eu^{+3} -doped ZnO was found to be slightly comparable to that of ZnO (3.22 eV) and also the direct band gaps are found to be approximately 3.19 eV.

4.3. Photoluminescence (PL)

Photoluminescence is produced from a semiconductor materials when excited electrons in higher energy level back to lower energy level by the releasing of energy difference via photon emission (Tebyetekerwa et al., 2020). The instrument used in this study was a Fluorescence Spectrometer, here in principle this type of instrument when the samples experiencing internal energy transition by releasing photon energy before returns to ground state some amount of absorbed energy get released such that the emitted light has minimum energy than the absorbed light. The photoluminescence spectra for ZnO NPs and Eu^{+3} -doped ZnO (EZO) Nanocomposites are presented in Fig. 11. The spectral analysis was conducted at excitation wavelength of 325nm. As the information obtained from the spectra, the samples have broad emission spectrum from 360nm to 550nm. The near-band edge (NBE) emission peak occurred at 395nm, it is typical electron-hole recombination emission peak of ZnO(Kandasamy et al., 2024). The others additional three important emission peaks in the visible region are associated with internal imperfections of the interstitial of Zn and O (Zn_i and O_i), antisites (Zn_O , O_Zn) and vacancies (V_Zn , V_O) (Sedky et al., 2023).The violet emissions peaks at about (420-423nm) is related to an electron transition from donor level to the valence band of ZnO (H. Naseer & Iqbal, 2024). The blue emission peaks at about 441nm is due to an electron transition between acceptor levels and conduction band of ZnO. The green emission (484-486nm) related to the transition of electrons between vacancy of oxygen (V_O) and vacancy of zinc (V_Zn) (Gebretsadik et al., 2024). Moreover, Fig. 11. revealed the two important effect of Eu^{+3} -doped ZnO (EZO) Nanocomposite on emission peaks, those are shifting of peaks toward higher wavelength with increasing dopants concentration and reduction in intensity of peaks. A reduction in intensity confirms minimum electron-holes recombination rate (Gebretsadik et al., 2024). Furthermore, there is a slight shifting of spectrum to higher wavelength for the Eu^{+3} -doped ZnO (EZO) Nanocomposite compared to the ZnO.

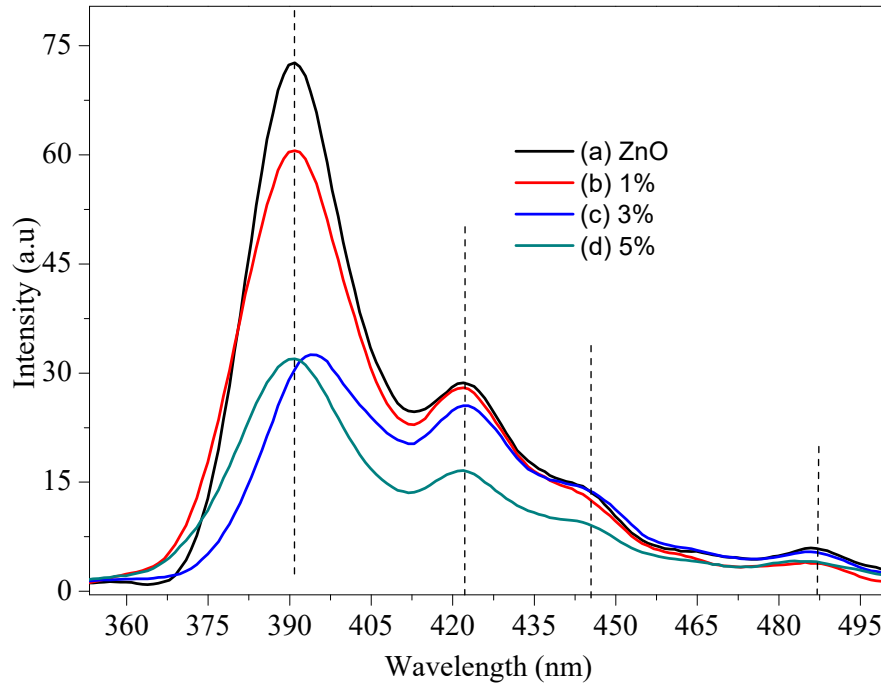


Figure 11: Photoluminescence spectra plot of ZnO and Eu^{+3} -doped ZnO (EZO) Nano composite. 1%, 3% and 5% represent the percentage of Eu^{+3} ions.

4.4. Fourier-Transform Infrared Spectroscopy (FTIR) Analysis

The functional group and chemical bonding information were investigated using the FTIR instrument, as depicted in Fig. 12. The band occurred at around 3500cm^{-1} is due to the O-H stretching vibration band associated to the interstitial or surface adsorbed water molecules. The metal-oxygen (M-O) bond bending vibration were detected in the fingerprint region, which is below 1000cm^{-1} are due to transverse optical stretching modes (Anžlovar et al., 2011). The strong absorption bands occurred at about 720cm^{-1} is due to the vibration of ZnO (Xiong et al., 2006). There are numerous bands occurred in the range of $3500-900\text{cm}^{-1}$, these maybe associated with the leftover impurities that appeared when the synthesis was conducted. The broad absorption band detected at 1450cm^{-1} is associated with the C-H bending vibration (Gemmech et al, 2022),

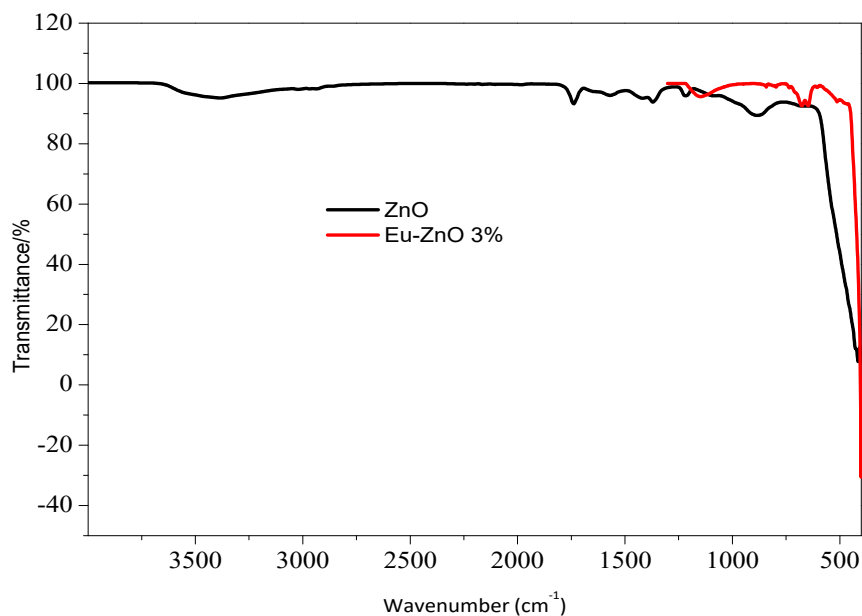


Figure 12: FTIR spectra plot of ZnO and Eu^{+3} -doped ZnO (EZO) Nanocomposite after calcinations of prepared samples.

4.5. Photocatalytic Activities

The photocatalytic degradation performance enhanced with the formation of more defects on the surface of porous nanomaterials (Sun et al., 2016). Recently, metal oxide semiconductor catalysts were playing important role in photocatalytic decomposition of methylene blue; ZnO has been studied widely for the decomposition of organic dyes (Khalid et al., 2023). It is certain that, during ZnO photocatalyst exposed to a light that have sufficient energy forms electron - holes pairs on the catalyst surface. The resulting holes interact with water producing strong oxidizing agent hydroxyl radicals ($\cdot\text{OH}$) and also the electrons react with oxygen provides super-oxide radicals, subsequently it forms more hydroxyl radicals (Cheng et al., 2020). Then, MB adsorbed on the photocatalyst, the hydroxyl radicals react with MB and converts to harmless products. Though, the issue of electron-hole recombination will be occurred when using ZnO NPs as a photocatalyst (Meky et al., 2023). The doping of rare earth elements is among the recent reasonable trial to solve these limitation of ZnO catalyst (Gebretsadik et al., 2024,).

The synthesized ZnO NPs and Eu^{+3} -doped ZnO (EZO) Nanocomposite were utilized as a photocatalyst for methylene blue degradation. The maximum absorption wavelength of methylene blue dye is at about 664nm. The degradation curve of methylene blue dye in aqueous solution by prepared photocatalysts is depicted in Fig. 13 and 15. The amount of

photocatalyst was kept 10mg in 10g/mL of Methylene blue and the experiment was conducted at pH about 10. Herein this study, an adsorption test was carried out in the dark condition for 30min. Thus, the samples were centrifuged and the absorbance was collected by UV-Vis spectrophotometer. When absorption of light carried out the blue color of methylene blue converts to colorless slowly as the time increases. Based on the information obtained from the graphs, the absorbance of solution in the presence of ZnO NPs was greater relative to other composites, which confirms the less degradation efficiency of ZnO ($k=0.025 \text{ min}^{-1}$) as compared to other composites. But, when ZnO was doped with different percentages of europium ion, the absorbance were decreased with the correlated amounts, which indicate excellent degradation ability of methylene blue dye. These improvement in degradation of methylene blue is related with the enhancement of absorption of light through doping of Europium ion (M. Kumar et al., 2021).

4.5.1. Percentage effect

The absorbances of suspension in the existence of different percentages of Europium dopant (1%, 3% and 5% EZO) was reduced compared to ZnO NPs, which confirms high degradation efficiency of blends. The enhanced photocatalytic efficiency of EZO due to visible light absorption advancement associated to dopants effect (Das et al., 2021). Moreover, the photocatalytic activity of EZO blends was reduced with the dopant amounts increased from 1% to 5% EZO, this is related to the formation of more defects on the ZnO crystals, which improves surface area and slightly disturbance crystallinity of catalysts (Hanh et al., 2024). Nano composites that have good crystallinity and larger surface area provides more active site for catalytic reaction center, ultimately the photocatalytic degradation efficiency was enhanced (Chong et al., 2024).

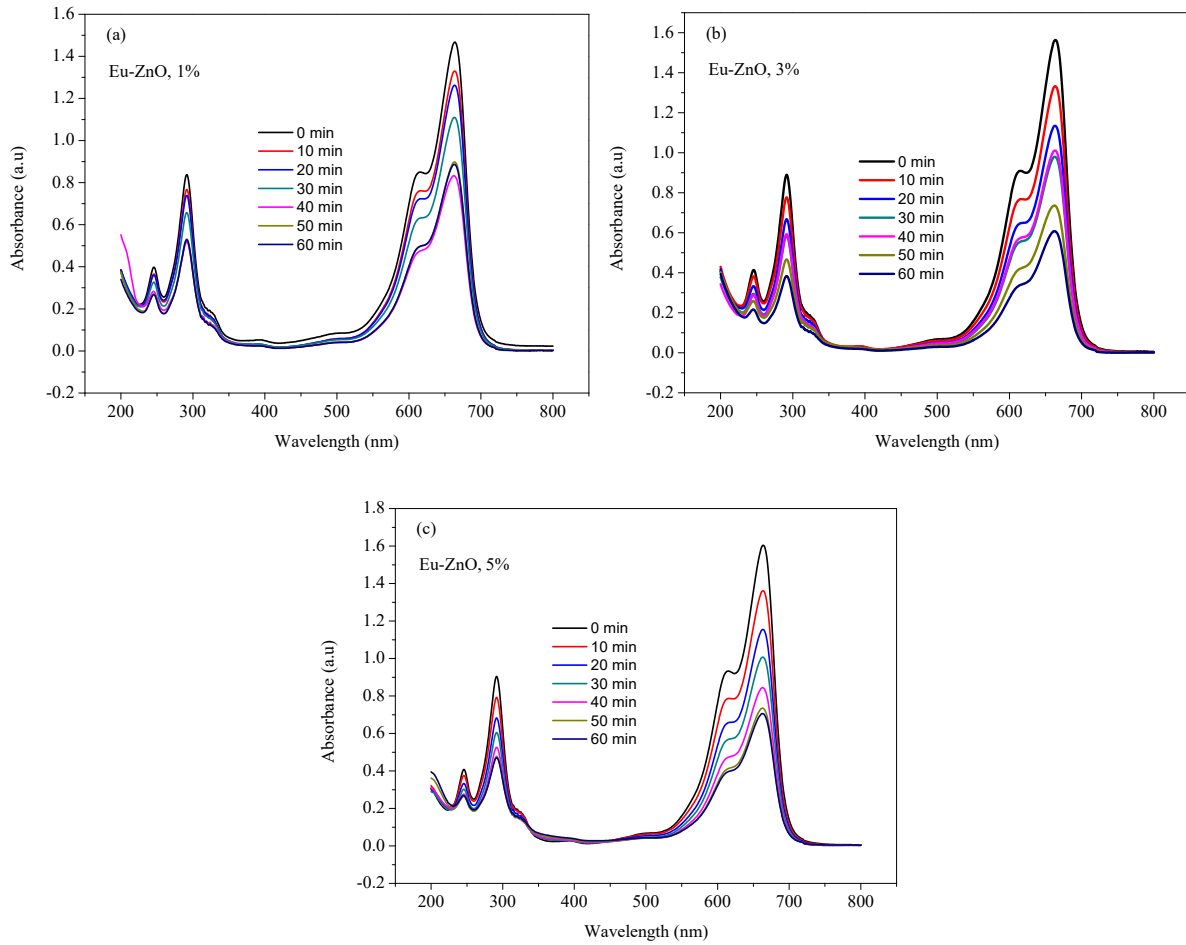


Figure 13: The percentage effect plots of absorbance versus wavelength (nm) of (a) 1% EZO, (b) 3% EZO, and (c) 5% EZO;

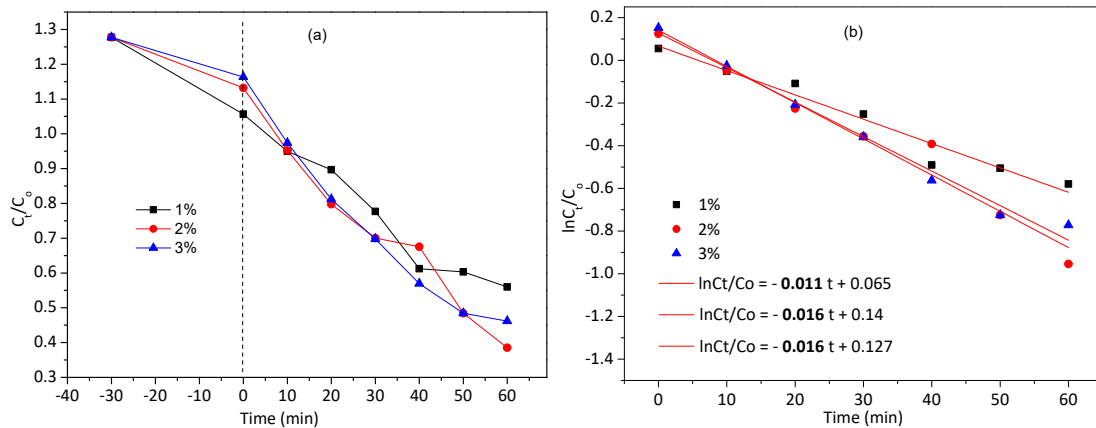
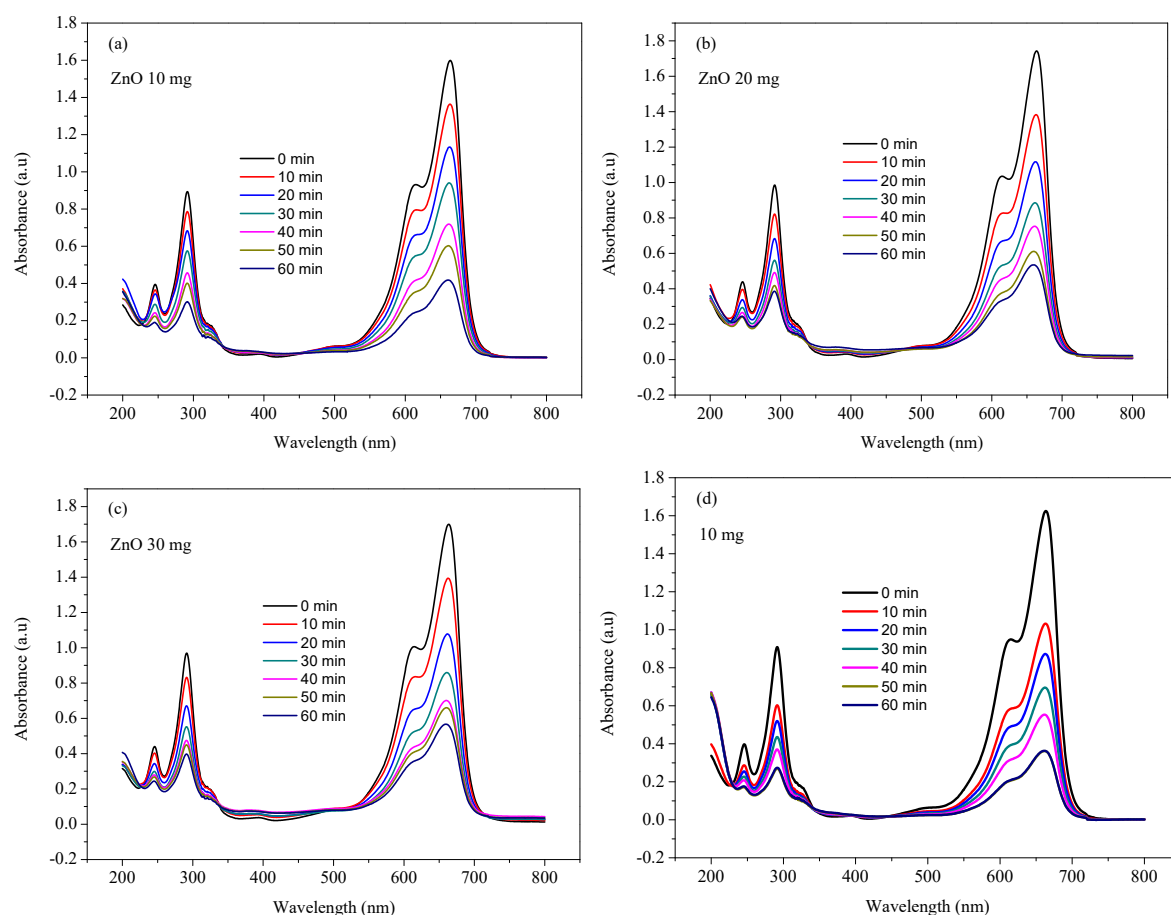


Figure 14: (a) the $\frac{C_t}{C_0}$ versus time (min) plot of different percentages of nanocomposites, (b) $\ln \frac{C_t}{C_0}$ versus time (min) plot of NPs and heterostructures

4.5.2. Dosage effect

The amount of photocatalyst is the considerable operational parameter in the photocatalytic degradation of pollutants(Ahmad et al., 2020). In this study, the dosage effect of ZnO NPs and EZO catalysts on photocatalytic degradation of MB was investigation as presented in Fig. 15 (a- f). As the dosage of ZnO or EZO photocatalyst increases beyond an optimal point, the rate constant decreases due to several factors. Higher catalyst loading leads to excessive light scattering and shielding, reducing the penetration of photons into the solution and limiting electron-hole pair generation. Moreover, agglomeration of particles at higher concentrations decreases the effective surface area and active sites, while increased turbidity causes mass transfer limitations. These combined effects lower photocatalytic efficiency, explaining the decrease in the reaction rate constant with excessive catalyst dosage(Akpan& Hameed, 2009), which decrease the number of active sites on the surface of catalyst that are open to light exposure.



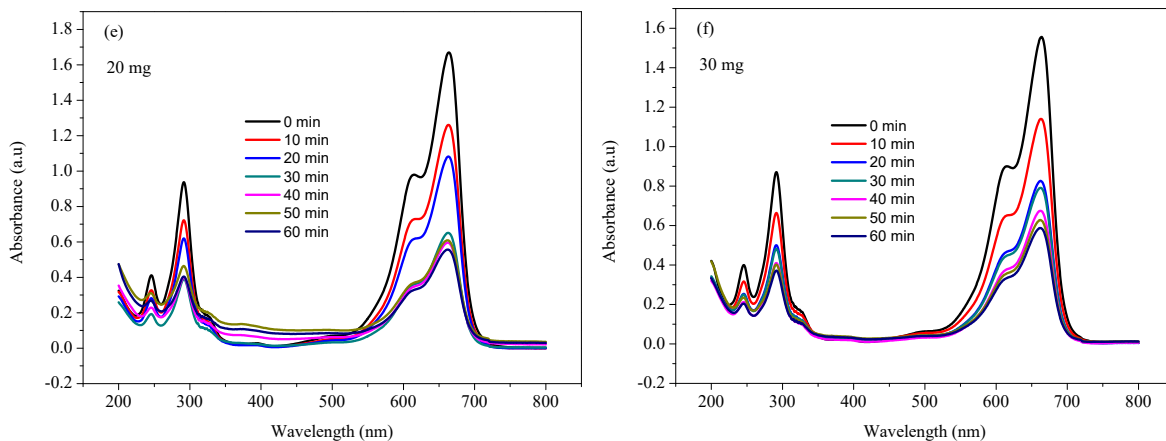


Figure 15: The dosage effect plots of absorbance versus wavelength (nm) of EZO nanocomposites; (a) 10 mg ZnO, (b) 20 mg ZnO, (c) 30 mg ZnO, (d) 10 mg 1% EZO, (e) 20 mg 3% EZO, and (f) 30 mg 5% EZO

The determination of the pseudo-first-order rate constant for degradation of methylene blue dye was conducted by plotting $\ln \frac{c_t}{c_0}$ versus irradiation time (Das et al., 2021). The graphs of $\ln \frac{c_t}{c_0}$ vs irradiation time as shown in Fig. 16, provides the rate constant for each photocatalysts from the slope of curves. The estimated rate constant for 10mg ZnO, 20mg ZnO, 30mg ZnONPs, 10 mg of 1% EZO, 20mg of 3% EZO, 20 mg of 5% EZO were found to be 0.025, 0.023, 0.021, 0.03, 0.02 and 0.01 min^{-1} .

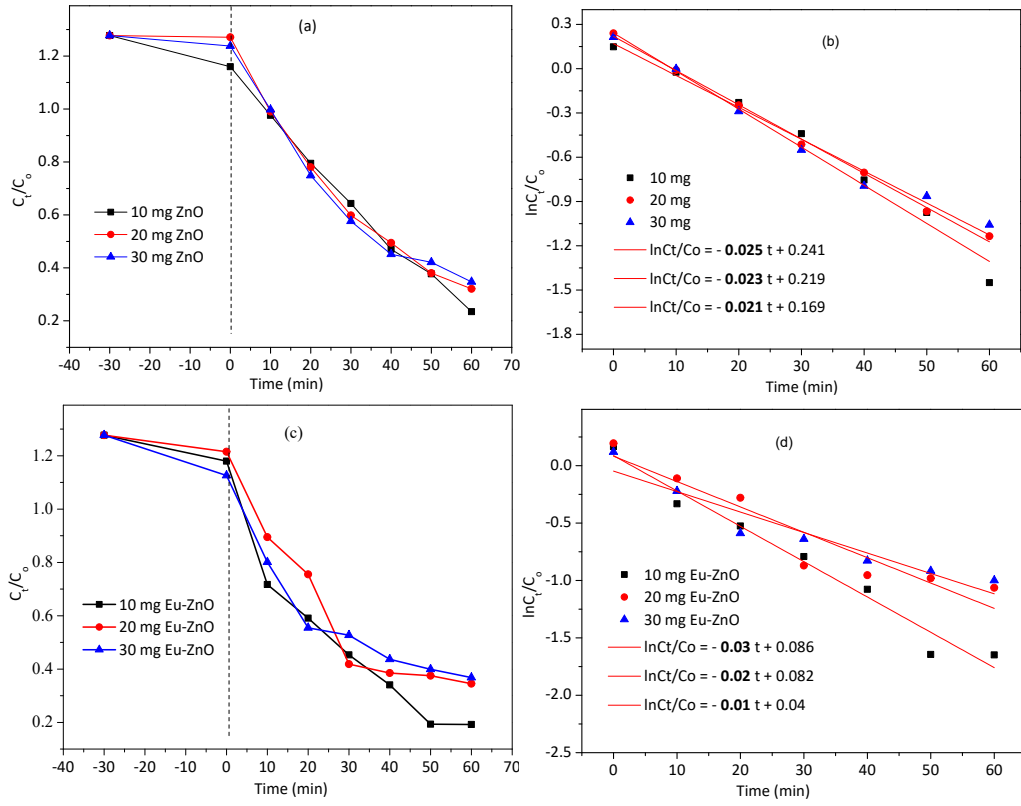


Figure 14: (a) the plots $\frac{C_t}{C_0}$ versus time (min) of NPs and composites, (b) $\ln \frac{C_t}{C_0}$ versus time (min) plot of NPs and composites

CHAPTER FIVE

5. CONCLUSION AND RECOMMENDATION

5.1. Conclusion

Here, a single phase hexagonal wurtzite ZnO and Eu⁺³-ZnO nanocomposite with the percentages of (1%, 3%, and 5%) were successfully synthesized using the simple solution combustion synthesis method. The effective doping of europium ions within the ZnO lattice is ensured by the shifting of ZnO XRD patterns and the disappearance of an independent europium oxide peak. UV-Visible diffuse reflectance spectroscopic and photoluminescence investigations confirmed the enhanced optical properties of ZnO through the doping of Europium. FTIR spectral analysis revealed the expected functional groups and chemical bonding in Eu⁺³-doped ZnO nanocomposites, typically the metal-oxygen bonds.

Finally, the photocatalytic degradation efficiency of the prepared sample was tested on methylene blue (MB) dye; Eu⁺³-doped ZnO nanocomposite ($k=0.3 \text{ min}^{-1}$) showed better photocatalytic degradation ability than single ZnO nanoparticles ($k=0.02 \text{ min}^{-1}$). This is associated to the advancement of ZnO optical properties through the incorporation of Europium ion within ZnO lattice.

5.2. Recommendation

According to the findings of this study, it is recommended that further research be carried out to optimize more operational parameter of photocatalytic degradation efficiency, the use of another types of dopants and the application of synthesized nanomaterials different areas such as biological activities (antibacterial, antifungal, anticancer) energy and sensors applications. This research tested only photocatalysis potential of prepared samples on real dye. Then, further research should be tested on dyes that are released from different factories and to be conducted on other type of synthetic dyes. In addition, to get more clear information about the formation of doping with metals, an advanced analytical technique like SEM, HR-TEM, and X-ray photoelectron spectroscopy (XPS) are advisable techniques. Besides, In order to ascertain which reactive species are typically involved in the photodegradation of the methylene blue dye, scavengers test is recommended to conduct that used during photoreaction.

REFERENCES

- Abebe, B., & Ananda Murthy, H. C. (2022). Insights into ZnO-based doped porous nanocrystal frameworks. *RSC Advances*, *12*(10), 5816–5833. <https://doi.org/10.1039/d1ra09152b>
- Abebe, B., Kefale, B., & Leku, D. T. (2023). Synthesis of copper-silver-zinc oxide nanocomposites for 4-nitrophenol reduction: doping and heterojunction. *RSC Advances*, *13*(7), 4523–4529. <https://doi.org/10.1039/d2ra07845g>
- Abebe, B., Tsegaye, D., & Ananda Murthy, H. C. (2022a). Insight into nanocrystal synthesis: from precursor decomposition to combustion. *RSC Advances*, *12*(37), 24374–24389. <https://doi.org/10.1039/D2RA05222A>
- Abebe, B., Tsegaye, D., & Ananda Murthy, H. C. (2022b). Insight into nanocrystal synthesis: from precursor decomposition to combustion. *RSC Advances*, *12*(37), 24374–24389. <https://doi.org/10.1039/d2ra05222a>
- Abebe, B., Tsegaye, D., Sori, C., Renuka Prasad, R. C. kuppe, & Murthy, H. C. A. (2023). Cu/CuO-Doped ZnO Nanocomposites via Solution Combustion Synthesis for Catalytic 4-Nitrophenol Reduction. *ACS Omega*, *8*(10), 9597–9606. <https://doi.org/10.1021/acsomega.3c00141>
- Adeel, M., Saeed, M., Khan, I., Muneer, M., & Akram, N. (2021). Synthesis and Characterization of Co-ZnO and Evaluation of Its Photocatalytic Activity for Photodegradation of Methyl Orange. *ACS Omega*, *6*(2), 1426–1435. <https://doi.org/10.1021/acsomega.0c05092>
- Adhikari, S., Sarkar, D., & Madras, G. (2014). Synthesis and photocatalytic performance of quasi-fibrous ZnO. *RSC Advances*, *4*(99), 55807–55814. <https://doi.org/10.1039/c4ra09376c>
- Ahmad, A., Khan, N., Giri, B. S., Chowdhary, P., & Chaturvedi, P. (2020). Removal of methylene blue dye using rice husk, cow dung and sludge biochar: Characterization, application, and kinetic studies. *Bioresource Technology*, *306*(March), 123202. <https://doi.org/10.1016/j.biortech.2020.123202>
- Akhmal Saadon, S., Sathishkumar, P., Mohd Yusoff, A. R., Hakim Wirzal, M. D., Rahmalan, M. T., & Nur, H. (2016). Photocatalytic activity and reusability of ZnO layer synthesised by electrolysis, hydrogen peroxide and heat treatment. *Environmental Technology (United Kingdom)*, *37*(15), 1875–1882. <https://doi.org/10.1080/09593330.2015.1135989>
- Akpan, U. G., & Hameed, B. H. (2009). Parameters affecting the photocatalytic degradation of dyes using TiO₂-based photocatalysts: A review. *Journal of Hazardous Materials*, *170*(2–3), 520–529. <https://doi.org/10.1016/j.jhazmat.2009.05.039>
- Al Rifai, S. A., & Kulnitskiy, B. A. (2013). Microstructural and optical properties of europium-doped zinc oxide nanowires. *Journal of Physics and Chemistry of Solids*, *74*(12), 1733–1738. <https://doi.org/10.1016/j.jpcs.2013.06.019>
- Alanazi, H. S., Ahmad, N., & Alharthi, F. A. (2021). Synthesis of Gd/N co-doped ZnO for

- enhanced UV-vis and direct solar-light-driven photocatalytic degradation. *RSC Advances*, 11(17), 10194–10202. <https://doi.org/10.1039/d0ra10698d>
- Albert manoharan, A., Chandramohan, R., Arun Kumar, K. D., Valanarasu, S., Ganesh, V., Shkir, M., Algarni, H., & AlFaify, S. (2018). Transition metal (Mn) and rare earth (Nd) di-doped novel ZnO nanoparticles: a facile sol–gel synthesis and characterization. *Journal of Materials Science: Materials in Electronics*, 29(15), 13077–13086. <https://doi.org/10.1007/s10854-018-9430-4>
- Anžlovar, A., Kogej, K., Crnjak Orel, Z., & Žigon, M. (2011). Polyol mediated nano size zinc oxide and nanocomposites with poly(methyl methacrylate). *Express Polymer Letters*, 5(7), 604–619. <https://doi.org/10.3144/expresspolymlett.2011.59>
- Applications, P. (2022). *Nano Biomed Eng Synthesis Europium (Eu 3 +) Doped Zinc Oxide Nanoparticles via the Co-Precipitation Method for*. 14, 58–70. <https://doi.org/10.5101/nbe.v14i1.p58-70>. Gemechu
- Armelaio, L., Bottaro, G., Pascolini, M., Sessolo, M., Tondello, E., Bettinelli, M., & Speghini, A. (2008). Structure-luminescence correlations in europium-doped sol-gel ZnO nanopowders. *Journal of Physical Chemistry C*, 112(11), 4049–4054. <https://doi.org/10.1021/jp710207r>
- Balapure, A., Ray Dutta, J., & Ganesan, R. (2024). Recent advances in semiconductor heterojunctions: a detailed review of the fundamentals of photocatalysis, charge transfer mechanism and materials. *RSC Applied Interfaces*, 1(1), 43–69. <https://doi.org/10.1039/d3lf00126a>
- Chen, P., Tai, Y., Fang, Q., Xu, D., Gao, Y., & Cheng, J. (2021). Solution combustion synthesis of ternary Ni/WC/C composites with efficient electrocatalytic oxygen reduction performance. *RSC Advances*, 11(61), 38718–38726. <https://doi.org/10.1039/d1ra06884a>
- Cheng, J., Zhan, C., Wu, J., Cui, Z., Si, J., Wang, Q., Peng, X., & Turng, L. S. (2020). Highly Efficient Removal of Methylene Blue Dye from an Aqueous Solution Using Cellulose Acetate Nanofibrous Membranes Modified by Polydopamine. *ACS Omega*, 5(10), 5389–5400. <https://doi.org/10.1021/acsomega.9b04425>
- Chong, C. Y., Sum, J. Y., Lai, L. S., Toh, P. Y., & Chang, Z. H. (2024). Visible light-driven dye degradation by magnetic cobalt-doped zinc oxide/iron oxide photocatalyst. *Next Materials*, 2(September 2023), 100074. <https://doi.org/10.1016/j.nxmte.2023.100074>
- Collivignarelli, M. C., Abbà, A., Carnevale Miino, M., & Damiani, S. (2019). Treatments for color removal from wastewater: State of the art. *Journal of Environmental Management*, 236(October 2018), 727–745. <https://doi.org/10.1016/j.jenvman.2018.11.094>
- Das, A., Patra, M., Kumar P, M., Bhagavathiachari, M., & Nair, R. G. (2021). Role of type II heterojunction in ZnO–In₂O₃ nanodiscs for enhanced visible-light photocatalysis through the synergy of effective charge carrier separation and charge transport. *Materials Chemistry and Physics*, 263(February), 124431. <https://doi.org/10.1016/j.matchemphys.2021.124431>
- Domingues, L., Jayakrishnan, A. R., Kaim, A., Gwozdz, K., Istrate, M. C., Ghica, C., Pereira, M., Castro, A., Marques, L., Hoye, R. L. Z., MacManus-Driscoll, J. L., & Silva, J. P. B.

- (2024). Tri-layered Si/Co₃O₄/ZnO heterojunction for high-performance visible photodetection. *Journal of Materials Chemistry C*, *12*(24), 8727–8736. <https://doi.org/10.1039/d4tc01624f>
- El Jouad, M., Bouabdalli, E. M., Touhtouh, S., Addou, M., Ollier, N., & Sahraoui, B. (2020). Red luminescence and UV light generation of europium doped zinc oxide thin films for optoelectronic applications. *EPJ Applied Physics*, *91*(1), 1–7. <https://doi.org/10.1051/epjap/2020200133>
- Gebretsadik, A., Kefale, B., Sori, C., Tsegaye, D., Ananda Murthy, H. C., & Abebe, B. (2024). Cu-doped ZnO/Ag/CuO heterostructure: superior photocatalysis and charge transfer. *RSC Advances*, *14*(41), 29763–29773. <https://doi.org/10.1039/d4ra05989a>
- Hamad, H. N., & Idrus, S. (2022). Recent Developments in the Application of Bio-Waste-Derived Adsorbents for the Removal of Methylene Blue from Wastewater: A Review. *Polymers*, *14*(4). <https://doi.org/10.3390/polym14040783>
- Hanh, N. H., Thi Minh Nguyet, Q., Van Chinh, T., Duong, L. D., Xuan Tien, T., Van Duy, L., & Hoa, N. D. (2024). Enhanced photocatalytic efficiency of porous ZnO coral-like nanoplates for organic dye degradation. *RSC Advances*, *14*(21), 14672–14679. <https://doi.org/10.1039/d4ra01345j>
- Iqbal, P., Preece, J. A., & Mendes, P. M. (2012). Nanotechnology: The “Top-Down” and “Bottom-Up” Approaches. *Supramolecular Chemistry*. <https://doi.org/10.1002/9780470661345.smc195>
- Joy, A., Viswanathan, M. R., Vijayan, B. K., Silva, C. G., Basheer, I., Sugathan, S., Mohamed, P. A., Solaiappan, A., & Shereef, A. (2024). Solar photocatalysts: non-metal (C, N, and S)-doped ZnO synthesized through an industrially sustainable in situ approach for environmental remediation applications. *RSC Advances*, *14*(30), 21655–21667. <https://doi.org/10.1039/d4ra03492a>
- Kandasamy, M., Husain, A., Suresh, S., Giri, J., Jasim, D. J., Rameshkumar, P., Al-Lohedan, H. A., Thambidurai, S., Kumar, N., Ansari, M. N. M., & Murugesan, S. (2024). Enhanced dye-sensitized solar cell performance and electrochemical capacitive behavior of bi-functional ZnO/NiO/Co₃O₄ ternary nanocomposite prepared by chemical coprecipitation method. *Journal of Science: Advanced Materials and Devices*, *9*(2), 100726. <https://doi.org/10.1016/j.jsamd.2024.100726>
- Khalid, A., Ahmad, P., Memon, R., Gado, L. F., Khandaker, M. U., Almukhlifi, H. A., Modafar, Y., Bashir, N., Abida, O., Alshammari, F. A., & Timoumi, A. (2023). Structural, Optical, and Renewable Energy-Assisted Photocatalytic Dye Degradation Studies of ZnO, CuZnO, and CoZnO Nanostructures for Wastewater Treatment. *Separations*, *10*(3). <https://doi.org/10.3390/separations10030184>
- Khin, M. M., Nair, A. S., Babu, V. J., Murugan, R., & Ramakrishna, S. (2012). A review on nanomaterials for environmental remediation. *Energy and Environmental Science*, *5*(8), 8075–8109. <https://doi.org/10.1039/c2ee21818f>
- Klingshirn, C., Fallert, J., Zhou, H., Sartor, J., Thiele, C., Maier-Flaig, F., Schneider, D., & Kalt, H. (2010). 65 years of ZnO research - old and very recent results. *Physica Status Solidi (B) Basic Research*, *247*(6), 1424–1447. <https://doi.org/10.1002/pssb.200983195>

- Koduru, J. R., Karri, R. R., & Mubarak, N. M. (2019). Smart materials, magnetic graphene oxide-based nanocomposites for sustainable water purification. *Sustainable Polymer Composites and Nanocomposites*, 759–781. https://doi.org/10.1007/978-3-030-05399-4_26
- Köhler, M., & Fritzsche, W. (2008). *Nanotechnology: an introduction to nanostructuring techniques*. John Wiley & Sons.
- Kshirsagar, S. D., Shelake, S. P., Biswas, B., Ramesh, K., Gaur, R., Abraham, B. M., Sainath, A. V. S., & Pal, U. (2024). Emerging ZnO Semiconductors for Photocatalytic CO₂ Reduction to Methanol. *Small*, 20(50). <https://doi.org/10.1002/sml.202407318>
- Kumar, M., Singh, G., & Chauhan, M. S. (2021). Europium (Eu³⁺) - doped ZnO nanostructures: Synthesis, characterization, and photocatalytic, chemical sensing and preliminary assessment of magnetic properties. *Ceramics International*, 47(12), 17023–17033. <https://doi.org/10.1016/j.ceramint.2021.03.008>
- Kumar, R., & Dosanjh, H. S. (2022). A mini-review on rare earth metal doped ZnO nanomaterials for photocatalytic remediation of waste water. *Journal of Physics: Conference Series*, 2267(1). <https://doi.org/10.1088/1742-6596/2267/1/012139>
- Lam, S. M., Sin, J. C., Abdullah, A. Z., & Mohamed, A. R. (2012). Degradation of wastewaters containing organic dyes photocatalysed by zinc oxide: A review. *Desalination and Water Treatment*, 41(1–3), 131–169. <https://doi.org/10.1080/19443994.2012.664698>
- Liu, Y., Zhang, X., Wu, B., Zhao, H., Zhang, W., Shan, C., Yang, J., & Liu, Q. (2019). Preparation Of ZnO/Co₃O₄ Hollow Microsphere By Pollen-biological Template And Its Application In Photocatalytic Degradation. *ChemistrySelect*, 4(43), 12445–12454. <https://doi.org/10.1002/slct.201903620>
- Magana-Arachchi, D. N., & Wanigatunge, R. P. (2020). Ubiquitous waterborne pathogens. In *Waterborne pathogens* (pp. 15–42). Elsevier.
- Meky, A. I., Hassaan, M. A., Fetouh, H. A., Ismail, A. M., & El Nemr, A. (2023). Cube-shaped Cobalt-doped zinc oxide nanoparticles with increased visible-light-driven photocatalytic activity achieved by green co-precipitation synthesis. *Scientific Reports*, 13(1), 1–24. <https://doi.org/10.1038/s41598-023-46464-7>
- Mengistu, A., Naimuddin, M., & Abebe, B. (2023). Optically amended biosynthesized crystalline copper-doped ZnO for enhanced antibacterial activity. *RSC Advances*, 13(35), 24835–24845. <https://doi.org/10.1039/d3ra04488b>
- Mishra, L., Paul, K. K., & Jena, S. (2021). Coke wastewater treatment methods: Mini review. *Journal of the Indian Chemical Society*, 98(10), 100133. <https://doi.org/https://doi.org/10.1016/j.jics.2021.100133>
- Mohammed, A., Abouzied, A. S., Albarakati, S., Algarni, M., Alotaibi, S. B., Alrahili, M. R., Reddy, S. G., & Abebe, B. (2025). Synthesis of Co-ZnO/Ag heterostructure for pollutant catalytic reduction: Interfacial electron transfer. *Inorganic Chemistry Communications*, 115050.

- Molavi, H., Mirzaei, K., Jafarpour, E., Mohammadi, A., Salimi, M. S., Rezakazemi, M., Nadagouda, M. M., & Aminabhavi, T. M. (2024). Wastewater treatment using nanodiamond and related materials. *Journal of Environmental Management*, 349(9), 119349. <https://doi.org/10.1016/j.jenvman.2023.119349>
- Mondal, S., Rana, U., Das, P., & Malik, S. (2019). Network of Polyaniline Nanotubes for Wastewater Treatment and Oil/Water Separation [Research-article]. *ACS Applied Polymer Materials*, 1(7), 1624–1633. <https://doi.org/10.1021/acscapm.9b00199>
- Mudalige, T., Qu, H., Van Haute, D., Ansar, S. M., Paredes, A., & Ingle, T. (2019). Characterization of nanomaterials: Tools and challenges. *Nanomaterials for Food Applications*, 313–353.
- Naseer, H., & Iqbal, T. (2024). Green synthesis of silver-doped zinc oxide nanoparticles for investigation of their photocatalytic activity and shelf life applications. *Biomass Conversion and Biorefinery*, 14(18), 21895–21911. <https://doi.org/10.1007/s13399-023-04380-w>
- Naseer, S., Aamir, M., Mirza, M. A., Jabeen, U., Tahir, R., Malghani, M. N. K., & Wali, Q. (2022). Synthesis of Ni-Ag-ZnO solid solution nanoparticles for photoreduction and antimicrobial applications. *RSC Advances*, 12(13), 7661–7670. <https://doi.org/10.1039/d2ra00717g>
- Nersisyan, H. H., Lee, J. H., Ding, J.-R., Kim, K.-S., Manukyan, K. V., & Mukasyan, A. S. (2017). Combustion synthesis of zero-, one-, two- and three-dimensional nanostructures: Current trends and future perspectives. *Progress in Energy and Combustion Science*, 63, 79–118. <https://doi.org/10.1016/j.pecs.2017.07.002>
- Perego, C., Millini, R., & Millini, R. (2013). Porous materials in catalysis: Challenges for mesoporous materials. *Chemical Society Reviews*, 42(9), 3956–3976. <https://doi.org/10.1039/c2cs35244c>
- Policy, E. S. (2015). *EVENTS SCIENCE POLICY PCAST provides assessment of US Nanotechnology Initiative*. 40(February), 106–107.
- Puspitasari, P., Soepriyanto, O. R., Sasongko, M. I. N., DIka, J. W., & Andoko. (2018). Mechanical and physical properties of aluminium-silicon (Al-Si) casting alloys reinforced by Zinc Oxide (ZnO). *MATEC Web of Conferences*, 204. <https://doi.org/10.1051/mateconf/201820405003>
- Ray, A., Subudhi, S., Tripathy, S. P., Acharya, L., & Parida, K. (2022). MOF Derived C/N Co-Doped ZnO Modified through Facile In Situ Coupling with NixPy toward Photocatalytic H₂O₂ Production and H₂ Evolution Reaction. *Advanced Materials Interfaces*, 9(34), 1–14. <https://doi.org/10.1002/admi.202201440>
- Reed, K., Cormack, A., Kulkarni, A., Mayton, M., Sayle, D., Klaessig, F., & Stadler, B. (2014). Exploring the properties and applications of nanoceria: is there still plenty of room at the bottom? *Environmental Science: Nano*, 1(5), 390–405.
- Riggert, J., Humpe, A., Legler, T. J., & Wolf, C. (2001). *Influence on Coagulation and Cellular Contamination*. 41(January), 82–86.

- Rong, P., Jiang, Y. F., Wang, Q., Gu, M., Jiang, X. L., & Yu, Q. (2022). Photocatalytic degradation of methylene blue (MB) with Cu₁-ZnO single atom catalysts on graphene-coated flexible substrates. *Journal of Materials Chemistry A*, *10*(11), 6231–6241. <https://doi.org/10.1039/d1ta09954j>
- Sarkar Phyllis, A. K., Tortora, G., & Johnson, I. (2022). Photodegradation. *The Fairchild Books Dictionary of Textiles*. <https://doi.org/10.5040/9781501365072.12105>
- Saxena, V., Kumar, N., & Saxena, V. K. (2017). A comprehensive review on combustion and stability aspects of metal nanoparticles and its additive effect on diesel and biodiesel fuelled C.I. engine. *Renewable and Sustainable Energy Reviews*, *70*(June 2016), 563–588. <https://doi.org/10.1016/j.rser.2016.11.067>
- Sedky, A., Afify, N., Almohammed, A., Ibrahim, E. M. M., & Ali, A. M. (2023). Structural, optical, photoluminescence and magnetic investigation of doped and Co-doped ZnO nanoparticles. *Optical and Quantum Electronics*, *55*(5), 1–24. <https://doi.org/10.1007/s11082-023-04718-8>
- Siddique, F., Gonzalez-Cortes, S., Mirzaei, A., Xiao, T., Rafiq, M. A., & Zhang, X. (2022). Solution combustion synthesis: the relevant metrics for producing advanced and nanostructured photocatalysts. *Nanoscale*, *14*(33), 11806–11868. <https://doi.org/10.1039/d2nr02714c>
- Singh, D., Batoor, K. M., Hussain, S., Kumar, A., Aziz, Q. H., Sheri, F. S., Tariq, H., & Singh, P. (2024). Enhancement of the photocatalytic activity of rGO/NiO/Ag nanocomposite for degradation of methylene blue dye. *RSC Advances*, *14*(4), 2429–2438. <https://doi.org/10.1039/d3ra07000j>
- Sun, Y., Chen, L., Bao, Y., Zhang, Y., Wang, J., Fu, M., Wu, J., & Ye, D. (2016). The applications of morphology controlled ZnO in catalysis. *Catalysts*, *6*(12). <https://doi.org/10.3390/catal6120188>
- Tebyetekerwa, M., Zhang, J., Xu, Z., Truong, T. N., Yin, Z., Lu, Y., Ramakrishna, S., Macdonald, D., & Nguyen, H. T. (2020). Mechanisms and applications of steady-state photoluminescence spectroscopy in two-dimensional transition-metal dichalcogenides. *ACS Nano*, *14*(11), 14579–14604. <https://doi.org/10.1021/acsnano.0c08668>
- Thenarasu, G., & Sivasamy, A. (2013). Metal ion doped semiconductor metal oxide nanosphere particles prepared by soft chemical method and its visible light photocatalytic activity in degradation of phenol. *Powder Technology*, *250*, 1–12. <https://doi.org/10.1016/j.powtec.2013.08.004>
- Vasyliov, G., Vorobyova, V., Skiba, M., & Khrokalo, L. (2020). Green synthesis of silver nanoparticles using waste products (apricot and black currant pomace) aqueous extracts and their characterization. *Advances in Materials Science and Engineering*, *2020*(1), 4505787.
- Wang, Z., Yang, X., Sun, C., Liu, H., Shao, J., Wang, M., Dong, J., Cao, G., & Pan, G. (2022). Excellent acetone sensing performance of Au NPs functionalized Co₃O₄-ZnO nanocomposite. *Sensor Review*, *42*(6), 638–647. <https://doi.org/10.1108/SR-12-2021-0486>

- Xia, P., Cao, S., Zhu, B., Liu, M., Shi, M., Yu, J., & Zhang, Y. (2020). Designing a 0D/2D S-Scheme Heterojunction over Polymeric Carbon Nitride for Visible-Light Photocatalytic Inactivation of Bacteria. *Angewandte Chemie - International Edition*, 59(13), 5218–5225. <https://doi.org/10.1002/anie.201916012>
- Xiong, G., Pal, U., Serrano, J. G., Ucer, K. B., & Williams, R. T. (2006). Photoluminescence and FTIR study of ZnO nanoparticles: The impurity and defect perspective. *Physica Status Solidi (C) Current Topics in Solid State Physics*, 3(10), 3577–3581. <https://doi.org/10.1002/pssc.200672164>
- Yang, Y., Li, Y., Zhu, L., He, H., Hu, L., Huang, J., Hu, F., He, B., & Ye, Z. (2013). Shape control of colloidal Mn doped ZnO nanocrystals and their visible light photocatalytic properties. *Nanoscale*, 5(21), 10461–10471. <https://doi.org/10.1039/c3nr03160h>
- Yin, Z., Li, S., Li, X., Shi, W., Liu, W., Gao, Z., Tao, M., Ma, C., & Liu, Y. (2023). A review on the synthesis of metal oxide nanomaterials by microwave induced solution combustion. *RSC Advances*, 13(5), 3265–3277. <https://doi.org/10.1039/d2ra07936d>